Modelling the light absorption properties of particulate matter forming organic particles suspended in seawater. Part 2. Modelling results*

OCEANOLOGIA, 47 (4), 2005.
pp. 621–662.

KEYWORDS
Organic particles
Suspended particulate matter
Light absorption coefficient
Imaginary part of the complex refractive index of light

Bogdan Woźniak[1,2,*]
Sławomir B. Woźniak[1,3]
Katarzyna Tyszka[1]
Mirosława Ostrowska[1]
Roman Majchrowski[2]
Dariusz Ficek[2]
Jerzy Dera[1]

[1] Institute of Oceanology,
Polish Academy of Sciences,
Powstańców Warszawy 55, PL–81–712 Sopot, Poland;

e-mail: wozniak@iopan.gda.pl

*corresponding author

[2] Institute of Physics,
Pomeranian Pedagogical Academy in Słupsk,
Arciszewskiego 22 B, PL–76–200 Słupsk, Poland

[3] Marine Physical Laboratory,
Scripps Institution of Oceanography,
University of California at San Diego,
La Jolla, 92093–0238 California, USA

Received 27 October 2005, revised 28 November 2005, accepted 1 December 2005.

* This work was carried out within the framework of IO PAS's statutory research, and also as part of project PZB–KBN 056/P04/2001/3 of the Institute of Physics, Pomeranian Pedagogical Academy in Słupsk.

Abstract

Model spectra of mass-specific absorption coefficients $a^*_{\mathrm{OM}}(\lambda)$ were established for 26 naturally occurring organic substances or their possible mixtures, capable of forming particulate organic matter (POM) in the sea. An algorithm was constructed, and the set of spectra of $a^*_{\mathrm{OM}}(\lambda)$ was used to determine the spectra of the imaginary part of the complex refractive index $n'_p(\lambda)$ characteristic of different physical types and chemical classes of POM commonly occurring in sea water. The variability in the spectra and absolute values of n'_p for the various model classes and types of POM was shown to range over many orders of magnitude. This implies that modelling the optical properties of sea water requires a multi-component approach that takes account of the numerous living and non-living fractions of POM, each of which has a different value of n'_p.

1. Introduction

This cycle of three articles aims to make a preliminary assessment of the spectral differentiation and the scale of variability of the absorption properties of suspended particles of organic matter in the sea (particulate organic matter – POM). The main focus here will be on the mean mass-specific absorption coefficients $a^*_{\mathrm{OM}}(\lambda)$[1] of unpackaged organic matter contained in various classes of organic particles, and the resultant absorption coefficients $a_{pm}(\lambda)$ of unpackaged particulate matter (organic and inorganic combined). Closely linked with these absorption coefficients is the imaginary part of the complex refractive index of light $n'_p(\lambda)$ of these particles (see eq. (2)). This index $n'_p(\lambda)$ can therefore also describe absorption and can be estimated as an alternative to $a_{pm}(\lambda)$. Our objective is to define the spectral characteristics typical of $n'_p(\lambda)$ for various sets and morphological types of particle occurring with a high degree of probability in sea waters.

As we already indicated in Part 1 of this cycle of articles (Woźniak et al. 2005a), achieving this objective by means of direct analyses and generalisations of the relevant empirical data is not possible at the moment because such data are unavailable. We do not have the relevant empirical sets of indices $a^*_{\mathrm{OM}}(\lambda)$, $a_{pm}(\lambda)$, and/or $n'_p(\lambda)$ for the various types of POM in the sea. Moreover, our knowledge of the structures of these particles is just as poor. This is why, for the purposes of this work, we have derived these indices indirectly from known mass-specific absorption coefficients of various naturally occurring organic substances which may be present in sea water and thus be a component of POM. Although we performed these calculations for model sets of marine organic particles distinguished largely

[1]This and other symbols for physical magnitudes and also the acronyms used in this paper are set out and explained in Appendix 1.

on the basis of theoretical speculations, we did nevertheless take a whole range of empirical premises derived from marine physics, chemistry and biology into consideration.

In Part 1 of this cycle (Woźniak et al. 2005a) we presented the principal results of the first phase of this study: (1) we distinguished 26 hypothetical model chemical classes and various physical types of POM on the basis of our knowledge of organic substances present in the marine environment; (2) some light absorption coefficients of the particulate material $a_{pm}(\lambda)$ and the associated imaginary refractive indices $n'_p(\lambda)$ were calculated for some of these chemical classes and physical types of model organic particles (oceanic phytoplankton pigments (*class P1*) and cells of live oceanic phytoplankton and phytoplankton-like particles (*class Ph1*)). Determining these latter optical parameters for the chemical *classes P1* and *Ph* was fairly straightforward, based as it was mainly on our knowledge of the chlorophyll-specific absorption coefficient of light for the entire set of oceanic phytoplankton pigments, and of the mass-specific light absorption coefficients of the individual pigments in this phytoplankton (see Woźniak et al. 1999, 2000, Majchrowski et al. 2000).

Now, in Part 2, which summarises the results of the second phase of research, we present a similar analysis of all the 26 hypothetical chemical classes of POM in the sea, including the oceanic phytoplankton cells and particles originating from oceanic phytoplankton that were analysed in Part 1 (i.e. *classes Ph1* and *P1*)[2]. Unfortunately, determining the resultant indices $a_{pm}(\lambda)$ and/or $n'_p(\lambda)$ for all these classes of POM turned out to be far more complicated than was the case with phytoplankton cells and phytoplankton-like particles. The relevant individual empirical mass-specific absorption coefficients of the many different organic substances making up the hypothetical classes of POM had to be gleaned from the literature. This process of selection, making preliminary inferences, and calculating the mean mass-specific absorption coefficients a^*_{OM} for the 26 chemical classes of POM were the main task in this second research phase (Part 2). This was completed thanks to the meticulous analyses and syntheses of numerous empirical data from the literature and from our own studies, the results of which we give here in section 2. Section 3 gives the algorithm for determining the resultant coefficients $a_{pm}(\lambda)$ and $n'_p(\lambda)$

[2]In Part 1, the analyses carried out for marine phytoplankton and the particles derived from it were more detailed. This was because we assumed the occurrence of various possible pigment compositions determined mainly by the light conditions in the water and its trophicity. Here, in contrast, the analyses have been done with respect to one pigment composition only, typical of the ocean, i.e. averaged over a variety of light conditions and trophicities.

mentioned earlier, which characterise the resultant absorption properties of unpackaged matter in organic particles for the model chemical classes and physical types. In section 4, this algorithm and the spectral runs of $a^*_{\mathrm{OM}}(\lambda)$ for the 26 model classes of POM (described in section 2) are used to determine and analyse the model spectra of $n'_p(\lambda)$ for these chemical classes and for the few physical types (including extreme types) of suspended particles most likely to occur in the sea. The probable range of variation of these spectra of $n'_p(\lambda)$ for most of these hypothetical classes and types of POM is also characterised here.

In Part 3 of this cycle we intend to show how these hypothetical classes and types of POM are linked with real morphological types of POM in the sea and to characterise the latter's absorption properties.

2. Mass-specific light absorption coefficients of the organic matter contained in particles

We have divided the 26 chemical classes of POM distinguished in Part 1 (Woźniak et al. 2005a) into the following three groups: (1) particles containing one organic component, (2) particles consisting of organic humus matter and (3) multi-component particles of organic matter (see Table 1 in Part 1). However, our description of the nature of each of these model chemical classes of particles in Part 1 was restricted to a definition of the composition and proportions by weight, and/or the origins, of the organic substances they contained. Expanding this description to include the spectral characteristics of the mean mass-specific absorption coefficients $a^*_{\mathrm{OM}}(\lambda)$ for the organic matter in these 26 chemical classes of particles (see Tables 1 and 2, also Fig. 1) only became possible at the present stage of our research.

In establishing the spectra of $a^*_{\mathrm{OM}}(\lambda)$ for the various chemical classes of particles, we utilised, among other things, the available empirical data on the individual absorption properties of selected organic compounds or their mixtures. We gleaned these data from the works of different authors, or else obtained them by generalising and averaging the empirical results of our own and others' studies. These data and their origins are discussed in the literature referred to in Tables 1 and 2. Here, then, we provide only the most important formal information explaining how we expanded the description of the nature of POM to include the mass-specific absorption coefficients of the organic matter contained in all 26 chemical classes of these particles. Our description is sub-divided in accordance with the three groups of POM mentioned above.

Table 1. List of chemical classes of model suspended organic particles in the sea and their mass-specific absorption coefficients

a – particles containing one organic component

Symbol	Name of class (kind of organic substance)	Mass-specific absorption coefficient [m^2 g^{-1}] and spectral range	Reference*
1	2	3	4
A1	Aromatic amino acids (protein fragments)	a^*_{A1} – values given in Table 2 (210–300 nm)	(A) and (1)
A2	Mycosporine-like amino acids (MAAs)	a^*_{A2} – values given in Table 2 (300–365 nm)	(2)
A3	Natural proteins	$a^*_{A3} = 0.93\exp(-0.00768(\lambda - 220)) + 0.075a^*_{A1}$ (T.1) (210–700 nm)	(2)
P1	Oceanic phytoplankton pigments	a^*_{P1} – values given in Table 2 (400–700 nm)	(3)
P2	Baltic phytoplankton pigments	a^*_{P2} – values given in Table 2 (380–700 nm)	(4)
N	Purine and pyridine compounds	a^*_N – values given in Table 2 (210–300 nm)	(A) and (5)
L	Lignins	a^*_L – values given in Table 2 (200–400 nm)	(6)

b – particles consisting of organic humic matter

1	2	3	4
H1	Baltic humus	a^*_{H1} – values given in Table 2 (200–600 nm)	(6)
H2	Atlantic coastal humus	$a^*_{H2} = 1.52\exp(-0.0175(\lambda - 400))$ (T.2) (300–525 nm)	(7)
H3	Humus from inland waters	$a^*_{H3} = 0.271\exp(-0.0111(\lambda - 400))$ (T.3) (200–700 nm)	(8)
H4	Marine humus	$a^*_{H4} = 0.125\exp(-0.0114(\lambda - 400))$ (T.4) (200–700 nm)	(8)
H5	Sargasso Sea humus	$a^*_{H5} = 0.165\exp(-0.02(\lambda - 400))$ (T.5) (300–525 nm)	(7)
H6, H7 and H8	Humus from the Gulf of Mexico	a^*_{H6} (or a^*_{H7} or a^*_{H8}) = $= fa^*_f + (1-f)a^*_h$ (T.6a) where f – degree of fulvisation (equal to 0, 1 and 0.9 for H6, H7 and H8 respectively), $a^*_f = 0.013\exp(-0.0184(\lambda - 400))$ (T.6b) $a^*_h = 0.228\exp(-0.011(\lambda - 400))$ (T.6c) (250–700 nm)	(9)
H9	Fulvic acids from Mississippi estuarine waters	$a^*_{H9} = 0.018\exp(-0.0194(\lambda - 400))$ (T.7) (250–700 nm)	(9)

Table 1. (*continued*)

b – particles consisting of organic humic matter (*continued*)

Symbol	Name of class (kind of organic substance)	Mass-specific absorption coefficient [m^2 g^{-1}] and spectral range	Reference*
H10	Soil humic acids	$a^*_{H10} = 0.58\exp(-0.009(\lambda - 400))$ (T.8) (VIS range)	(8)
H11	Soil fulvic acids	$a^*_{H11} = 0.29\exp(-0.011(\lambda - 400))$ (T.9) (VIS range)	(8)
H12	Humic acids from bottom sediments	$a^*_{H12} = 0.09\exp(-0.0095(\lambda - 400))$ (T.10) (VIS range)	(10)
H13	Fulvic acids from bottom sediments	$a^*_{H13} = 0.053\exp(-0.01475(\lambda - 400))$ (T.11) (VIS range)	(11)

c – multi-component particles of organic matter

1	2	3	4
Ph1	Oceanic phytoplankton and phytoplankton-like particles	$a^*_{Ph1} = 0.01(\Sigma C/C_a)a^*_{P1} + +(0.49 - 0.01\Sigma C_{acc}/C_a)a^*_{A3}$ (T.12) where $\Sigma C/C_a = 3.1$ and $\Sigma C_{acc}/C_a = 2.1$ (400–700 nm)	(A) (3) and (11)
Ph2	Baltic phytoplankton and phytoplankton-like particles	$a^*_{Ph2} = 0.01(\Sigma C/C_a)a^*_{P2} + +(0.49 - 0.01\Sigma C_{acc}/C_a)a^*_{A3}$ (T.13) where $\Sigma C/C_a = 5.3$ and $\Sigma C_{acc}/C_a = 4.3$ (400–700 nm)	(A) (4) and (11)
PhM	Polar phytoplankton and phytoplankton-like particles	a^*_{PhM} – values given in Table 2 (300–700 nm)	(2)
Z	Zooplankton and zooplankton-like and/or nekton-like particles	$a^*_Z = 0.7a^*_{A3}$ (T.14) (210–600 nm)	(A) and (11)
D1	Oceanic DOM-like particles	$a^*_{D1} = 0.012a^*_{A3} + +0.003a^*_N + 0.1a^*_{H4}$ (T.15) (210–600 nm)	(A)
D2	Baltic DOM-like particles	$a^*_{D2} = 0.08a^*_{A3} + 0.02a^*_N + +0.18a^*_L + 0.55a^*_{H1}$ (T.16) (210–700 nm)	(A)

* References: (1) Cambell & Dwek 1984; (2) Moisan & Mitchell 2001; (3) Woźniak et al. 1999; (4) Ficek et al. 2004; (5) Filipowicz & Więckowski 1983; (6) Nyquist 1979; (7) Stuermer 1975; (8) Zepp & Schlotzhaur 1981; (9) Carder et al. 1989; (10) Hayase & Tsubota 1985; (11) Romankevich 1977; (A) The composition and/or origin of organic substances in a particle was assumed on the basis of the author's own studies.

Table 2. Spectral mass-specific coefficients of light absorption for the compositions of organic matter analysed in this paper (data supplementary to those in Table 1)*

Wavelength [nm]	a^*_{A1}	a^*_{A2}	a^*_{P1}	a^*_{P2}	a^*_N	a^*_L	a^*_{H1}	a^*_{PhM}
	[m^2 g^{-1}]							
1	2	3	4	5	6	7	8	9
200						2.12E+01		
210	1.81E+01				1.29E+01	1.52E+01	8.00E+00	
220	2.12E+01				1.20E+01	9.00E+00	6.10E+00	
230	2.70E+00				6.30E+00	7.90E+00	5.10E+00	
240	7.00E–01				9.60E+00	5.30E+00	4.60E+00	
250	1.30E+00				1.26E+01	2.80E+00	3.90E+00	
260	1.80E+00				1.55E+01	2.20E+00	3.60E+00	
270	2.50E+00				1.72E+01	2.60E+00	3.30E+00	
280	2.40E+00				1.37E+01	2.80E+00	2.90E+00	
290	6.80E–01				9.10E+00	2.30E+00	2.60E+00	
300	7.00E–02	2.77E+02			2.10E+00	1.50E+00	2.20E+00	1.25E+00
305		2.44E+02						1.13E+00
310		2.33E+02				1.20E+00	1.90E+00	1.09E+00
315		2.35E+02						1.13E+00
320		2.59E+02				9.20E–01	1.60E+00	1.26E+00
325		2.99E+02						1.45E+00
330		3.48E+02				3.00E–01	1.46E+00	1.67E+00
335		3.64E+02						1.75E+00
340		3.58E+02				6.40E–01	1.20E+00	1.72E+00
345		3.35E+02						1.60E+00
350		2.92E+02				5.30E–01	1.05E+00	1.39E+00
355		2.17E+02						1.05E+00
360		1.47E+02				3.50E–01	9.00E–01	7.45E–01
365		1.03E+02						5.63E–01
370						2.10E–01	7.30E–01	4.89E–01
375								4.69E–01
380				6.03E+00		1.10E–01	6.20E–01	4.77E–01
385				6.32E+00				4.99E–01
390				6.54E+00		6.60E–02	5.30E–01	5.15E–01
395				6.68E+00				5.23E–01
400			1.60E+01	7.09E+00		5.50E–02	4.60E–01	5.27E–01
405				7.67E+00				5.41E–01
410			1.99E+01	8.45E+00				5.66E–01
415				8.91E+00				5.84E–01
420			2.52E+01	9.19E+00				5.83E–01
425				9.29E+00				5.85E–01
430			3.16E+01	9.64E+00				6.00E–01
435				1.01E+01				6.23E–01
440			3.61E+01	9.95E+00				6.29E–01
445				9.26E+00				6.11E–01
450			2.85E+01	8.31E+00			2.10E–01	5.87E–01
455				7.79E+00				5.75E–01
460			2.78E+01	7.57E+00				5.65E–01
465				7.35E+00				5.48E–01

Table 2. (*continued*)

1	2	3	4	5	6	7	8	9
470			2.70E+01	6.93E+00				5.24E–01
475				6.37E+00				4.96E–01
480			2.43E+01	5.97E+00				4.68E–01
485				5.76E+00				4.38E–01
490			2.29E+01	5.59E+00				3.98E–01
495				5.34E+00				3.53E–01
500			1.85E+01	4.92E+00			1.20E–01	3.05E–01
505				4.35E+00				2.61E–01
510			1.15E+01	3.83E+00				2.22E–01
515				3.37E+00				1.90E–01
520			7.10E+00	3.03E+00				1.65E–01
525				2.80E+00				1.42E–01
530			5.45E+00	2.66E+00				1.23E–01
535				2.50E+00				1.03E–01
540			4.74E+00	2.39E+00				8.57E–02
545				2.27E+00				7.23E–02
550			4.00E+00	2.15E+00			6.60E–02	6.08E–02
555				1.98E+00				5.20E–02
560			3.26E+00	1.84E+00				4.62E–02
565				1.70E+00				4.33E–02
570			2.68E+00	1.61E+00				4.40E–02
575				1.53E+00				4.78E–02
580			2.42E+00	1.39E+00				5.00E–02
585				1.37E+00				5.62E–02
590			2.52E+00	1.33E+00				6.07E–02
595				1.26E+00				6.15E–02
600			2.74E+00	1.20E+00			3.50E–02	5.92E–02
605				1.22E+00				5.54E–02
610			2.87E+00	1.28E+00				5.43E–02
615				1.40E+00				5.74E–02
620			3.00E+00	1.50E+00				6.01E–02
625				1.54E+00				6.11E–02
630			3.26E+00	1.59E+00				6.37E–02
635				1.60E+00				6.89E–02
640			3.74E+00	1.60E+00				7.34E–02
645				1.62E+00				7.38E–02
650			4.35E+00	1.70E+00			1.86E–02	7.63E–02
655				1.95E+00				8.60E–02
660			5.68E+00	2.51E+00				1.12E–01
665				3.41E+00				1.59E–01
670			9.16E+00	4.29E+00				2.07E–01
675				4.59E+00				2.19E–01
680			8.52E+00	4.21E+00				1.80E–01
685				3.18E+00				1.14E–01
690			3.87E+00	1.95E+00				5.78E–02
695				1.06E+00				2.59E–02
700			2.13E+00	5.98E–01			9.84E–03	1.09E–02

* The values for 650 and 750 nm in column 8 have been extrapolated on the basis of the spectral slopes on a logarithmic scale in the range from 550 to 600 nm.

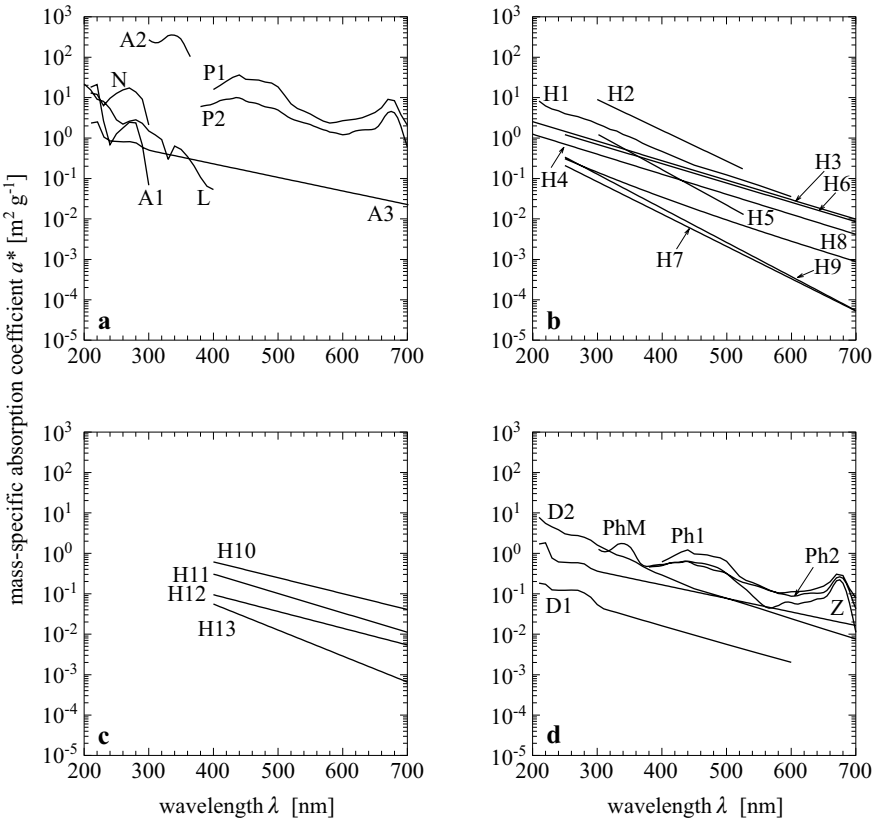

Fig. 1. Model spectra of mass-specific coefficients of light absorption by organic matter established for selected model chemical classes of POM: (a) single-component organic particles; (b) and (c) particles containing organic humus matter originating from the sea, and from the soil or bottom sediments, respectively; (d) multi-component organic particles (graphs plotted on the basis of calculations according to eqs. (T1)–(T16) contained in Table 1 or based on the data tabulated in Table 2. The symbols denoting the curves on the graphs correspond to the various chemical classes of particles, in line with the convention adopted in Table 1, columns 1 and 2)

2.1. Single-component organic particles

This group comprises the following seven classes of particles containing single-component organic matter and characterised by particularly strong UV and VIS absorption: (A1) Aromatic amino acids (protein-fragments); (A2) Mycosporine-like amino acids (MAAs); (A3) Natural proteins; (N) Purine and pyridine compounds; (P1) Oceanic phytoplankton pigments; (P2) Baltic phytoplankton pigments; (L) Lignins.

The term 'single-component matter' is purely a matter of convention and does not imply that a particle consists of one and only one chemical compound. What it does mean is that the matter containing organic compounds is classified in the same group of compounds. For example, a particle classified in group A1 (aromatic amino acids) may contain different aromatic amino acids, i.e. be a mixture of tryptophan, tyrosine and phenylalanine. Hence, the absorption properties of such single-component organic particles are in fact the resultant absorption properties of mixtures of the chemical constituents making up a given group of particles. The most important examples of such individual spectra of the mass-specific absorption coefficients of light for various component compounds, which were used, among other things, to determine the resultant absorption properties of the 26 chemical classes of POM, are given in Appendix 2 (Fig. A2.1). On the other hand, the resultant spectra of the mass-specific absorption coefficients for all the classes of particles containing one organic component are set out as an analytical record in Table 1a (see eqs. (T1) –(T16) in column 3 of this Table), or in tabular form (Table 2 [supplementary to Table 1], columns 2–7), for various wavelengths of light. Their graphs have been plotted in Fig. 1a. The resultant spectra for the various classes were established according to the principles outlined below.

– *Class A1.* The model spectral values of the mass-specific absorption coefficient of light $a^*_{A1}(\lambda)$ for POM containing aromatic amino acids (see Fig. 1a, curve A1), i.e. the strongest UV absorbers in the 200 –300 nm range among the amino acids were taken to be the respective arithmetic mean values of the mass-specific absorption coefficients of light $a^*_{A1}(\lambda)$ for the three aromatic amino acids biosynthesised in nature – tryptophan, tyrosine and phenylalanine (see Fig. A2.1a in Appendix 2).

– *Class A2.* In view of the lack of direct empirical data on the individual absorption properties of mycosporine-like amino acids (MAAs – mycosporine-glycine, shinorine and mycosporine-glycine valine, among others), the strongest known organic absorbers of UV in the 300–365 nm range, the mean values of their model spectral coefficient $a^*_{A2}(\lambda)$ (Fig. 1a, curve A2) were estimated indirectly. They were assumed to be approximately equal to the mass-specific absorption of a natural mixture of these compounds in *Phaeocystis antarctica* incubated under various irradiance conditions. To this end, we used the relevant experimental data kindly supplied by Dr T.A. Moisan, and also those extracted from Moisan & Mitchell (2001), compiled in the manner outlined in Appendix 3. This averaged model spectrum of $a^*_{A2}(\lambda)$ corresponds to a mixture of the three compounds

mentioned earlier: mycosporine-glycine, shinorine and mycosporine-glycine valine, which occur in the following (averaged) proportions by weight: 0.12:0.55:0.33.

– *Class A3.* In fixing the model spectrum of the coefficient $a^*_{A3}(\lambda)$ of natural proteins (i.e. a mixture of simple proteins and proteids), account was taken of the fact that its course is to a first approximation the effect of light absorption by all their component amino acids and possibly other submolecular components of proteids. From the optical standpoint, these compounds can, to a rough approximation, all be put into one or other of two groups (Filipowicz & Więckowski 1983): aromatic amino acids (mentioned above) and other compounds. The former are strong UV absorbers. The latter, mostly saturated amino acids (ammonium, amine or imine), absorb light less strongly[3], but do so in various UV and VIS spectral regions; also, they may occur only sporadically. Hence, the resultant spectral coefficients a^*_{A3} for proteins (shown in Fig. 1a, curve A3) were described as the sum of two such coefficients (see eq. (T1), column 3 in Table 1a), each derived from one of the two groups of absorbers named above. The first of them is the above-mentioned model spectrum of $a^*_{A1}(\lambda)$ for aromatic amino acids (*particle class A1*). It participates in the expression for the total absorption with an appropriate weight k (we estimated its value at $k = 0.075$), giving the mean ratio of the mass of all aromatic molecules in the peptide chain to the overall mass of the chain. The second component of this coefficient, responsible for light absorption by the other amino acids contained in various proteins and by other proteid components, was estimated from a curve decreasing exponentially with increasing light wavelength λ. The rough values of the parameters of this approximating curve were established on the basis of a statistical analysis of a set of more than a dozen empirical absorption spectra of various complex protein forms (see the examples in Fig. A2.1d).

– *Class N.* Three compounds – adenine, guanine and cytosine – were assumed to be the principal light absorbers in particle *class N*, (purine and pyridine compounds, nucleic acid fragments), since they strongly absorb UV radiation in the 200–300 nm band. Hence, the model spectrum of $a^*_N(\lambda)$, the mass-specific absorption coefficient of light by

[3]Except for MAAs, which are exceedingly strong absorbers of light in the 300–400 nm range. However, in nature they occur only sporadically: we did not find any literature reports confirming their occurrence on a large scale, or that they are common throughout the World Ocean. Be that as it may, they undoubtedly are present in regions exposed to elevated levels of natural UV radiation, e.g. in the Arctic and Antarctic (see e.g. Garcia-Pichel 1994, Vernet & Whitehead 1996).

the organic matter in these particles, was determined by averaging the relevant empirical coefficients (Fig. A2.1c) for these three compounds mixed in proportions by weight of 1:1:1. This model spectrum of $a^*_N(\lambda)$ is illustrated in Fig. 1a – curve N.

– *Class P1* and *class P2*. It was assumed that the organic matter contained by the particles in these two classes would consist of various phytoplankton pigments (photosynthetic and photoprotecting). They are some of the strongest absorbers of VIS light (see Figs A2.1e and A2.1f) and occur in the proportions typical of oceanic phytoplankton (*class P1*) or of Baltic phytoplankton (*class P2*). Therefore the model coefficients a^*_{P1} for the class of oceanic phytoplankton pigments were assumed to take the mean values of the mass-specific absorption coefficient of light by all phytoplankton pigments in the 'in solvent' state. We had defined them earlier by averaging a set of 122 empirical spectra of the chlorophyll-specific absorption coefficient by phytoplankton from various oceanic case 1 waters, after having eliminated the pigment packaging effect (after Woźniak et al. 1999 – see Fig. 3a in that paper), and converting the chlorophyll-specific absorption to mass-specific absorption (i.e. with respect to the mass of all pigments). In the same way, the model coefficients a^*_{P2} for the 'Baltic' pigments were determined from similar analyses of 817 empirical spectra of light absorption by phytoplankton from different parts of the Baltic (after Ficek et al. 2004, see Fig. 2b). The model spectra of $a^*_{P1}(\lambda)$ and $a^*_{P2}(\lambda)$ are shown in Fig. 1a – curves P1 and P2.

– *Class L*. Unlike the above spectra of mass-specific absorption coefficients for six classes of homogeneous organic particles, derived indirectly by averaging, the spectra for *class L* were based on direct measurements. This class encompassed lignin-containing particles absorbing UV, and the model values of their mass-specific absorption coefficients a^*_L were based on measurements made for lignins isolated from Baltic waters (Nyquist 1979) (Fig. 1a, curve L).

2.2. Particles containing organic humus matter

This group of POM consists of 13 chemical classes of particles containing autogenic or allogenic humus matter which are fairly strong UV and VIS absorbers: (H1) Baltic humus; (H2) Atlantic coastal humus; (H3) humus from inland waters; (H4) marine humus; (H5) Sargasso Sea humus; (H6, H7, and H8) – humus from Gulf of Mexico waters, consisting of mixtures of the same humus acids (humic and fulvic acids) but differing in their degree

of fulvisation[4], which for these three classes is 0, 0.1 and 0.9 respectively; (H9) fulvic acids from Mississippi estuarine waters; (H10) soil humic acids; (H11) soil fulvic acids; (H12) humic acids from bottom sediments; (H13) fulvic acids from bottom sediments.

In establishing the model spectra of the mass-specific absorption coefficients $a^*_{H1}(\lambda)$ – $a^*_{H13}(\lambda)$ for all 13 classes (see Table 1b) we took into consideration direct measurements by various authors (see Table 1b, column 4) made on samples of unseparated humus, or separately on fulvic acid and humic acid fractions isolated from various sea and inland waters (*classes H1–H9*), and from soils and bottom sediments (*classes H10–H13*). Since these spectra usually display a monotonic decrease in absorption with increasing wavelength, many of them have been approximated by means of exponential functions (see eqs. (T.2)–(T.11) in Table 1b, column 3), or are shown in tabular form (Table 2, column 8). These spectra are illustrated graphically, separately for humus from aquatic environments (Fig. 1b – curves H1 to H9) and for humus from soils and bottom sediments (Fig. 1c – curves H10 to H13).

2.3. Multi-component organic particles

This group of POM contains 6 chemical classes of particles, the organic matter of which includes organic compounds that are strong UV and/or VIS absorbers: (Ph1) oceanic phytoplankton cells and oceanic phytoplankton-like particles; (Ph2) Baltic phytoplankton cells and Baltic phytoplankton-like particles; (PhM) polar phytoplankton cells and polar phytoplankton-like particles; (Z) zooplankton cells, zooplankton and/or nekton-like particles; (D1) oceanic DOM-like particles; (D2) Baltic DOM-like particles.

The organic matter of such multi-component particles consists of simpler organic substances (for convenience denoted by the subscript i – see eq. (1)), the spectra of whose mass-specific absorption coefficients $a^*_{\mathrm{OM},i}(\lambda)$ were discussed above (subsections 2.1 and 2.2) and are set out in Tables 1a, 1b and 2. Hence, the resultant spectra of the mass-specific absorption coefficient $a^*_{\mathrm{OM}}(\lambda)$ of multi-component particles can be determined by averaging the light absorption spectra of the various components of the particles $a^*_{\mathrm{OM},i}(\lambda)$, according to the relationship:

$$a^*_{\mathrm{OM}}(\lambda) = \frac{1}{C_{\mathrm{OM}}} \Sigma_i a^*_{\mathrm{OM},i}(\lambda) C_{\mathrm{OM},i}, \tag{1}$$

where $C_{\mathrm{OM},i}$ stands for the concentrations of the particular components, and C_{OM} their sum, i.e. the combined intracellular organic matter concentration.

[4]By the degree of fulvisation is meant (after Carder et al. 1989) the ratio of the mass of fulvic acids to the total mass, i.e. the combined mass of fulvic and humic acids.

Equation (1) was used to define the model absorption spectra of $a^*_{\mathrm{OM}}(\lambda)$: $a^*_{Ph1}(\lambda)$, $a^*_{Ph2}(\lambda)$, $a^*_Z(\lambda)$, $a^*_{D1}(\lambda)$, and $a^*_{D2}(\lambda)$, that is, for 5 of the 6 model classes of multi-component particles. In doing so, the approximate proportions between the concentrations of the various organic components of these particles, regarded as typical and discussed in Part 1[5] (see Table 1c in Woźniak et al. 2005), were taken into consideration. It was further assumed that $a^*_{\mathrm{OM},i}(\lambda) = 0$ for the remaining organic matter that does not absorb light. Given these assumptions, particular cases of eq. (1) that apply to model spectra of $a^*_{\mathrm{OM}}(\lambda)$ for particular particle classes take the forms presented in Table 1c (see eqs. (T.12)–(T.16) in column 3 of that Table). These spectra, interpolated and extrapolated, are illustrated in Fig. 1d (see curves Ph1, Ph2, Z, D1 and D2).

On the other hand, the spectrum of $a^*_{PhM}(\lambda)$ for *class PhM* (polar phytoplankton and polar phytoplankton-like particles) was determined not by summing and averaging, but, as was done with the MAAs (subsection 2.1), on the basis of direct measurements (Moisan & Mitchell 2001) (for an explanation – see Appendix 3). The values of this coefficient for different wavelengths are given in Table 2 (column 9), and the spectra are presented graphically by curve PhM in Fig. 1d.

3. Method of calculating the imaginary refractive indices for model particles of organic matter suspended in the sea

An alternative way of describing the resultant absorption properties of POM is by means of the spectrum of the light absorption coefficient for particulate matter $a_{pm}(\lambda)$, or the spectrum of the imaginary part of the complex refractive index of these particles $n'_p(\lambda)$. This alternative emerges from the fact that these coefficients are linked by the relationship (Born & Wolf 1968, Van de Hulst 1981):

$$n'_p(\lambda) = \frac{\lambda}{4\pi}\, a_{pm}(\lambda). \tag{2}$$

As we can see, the values $a_{pm}(\lambda)$ and $n'_p(\lambda)$ are equivalent, differing only in the factor $\lambda/4\pi$, which is dependent on the light wavelength λ. That is why the imaginary refractive index of a material is defined as its dimensionless coefficient of light absorption. Thus, to describe these resultant absorption properties of unpackaged particulate matter in this

[5]It is worth explaining that when establishing these approximate compositions of organic matter in particles of *classes Ph1*, *Ph2* and *Z*, we took account of the typical biogeochemical compositions of marine organisms, given in Appendix 4. On the other hand, we based our assumption of similar organic matter compositions for *classes D1* and *D2* on a review of literature papers, too numerous to mention here, and on the as yet unpublished results of our own studies.

paper (see section 4) we have used only one of these coefficients, namely, the imaginary refractive index $n'_p(\lambda)$.

Now we shall move on to the algorithm for calculating the two coefficients $a_{pm}(\lambda)$ and $n'_p(\lambda)$ (subsection 3.1) from known coefficients $a^*_{\mathrm{OM}}(\lambda)$. Then we shall discuss the relevant physical constants assumed in the algorithm (subsection 3.2) and the input data required to perform such calculations (subsection 3.3).

3.1. The algorithm

Let us assume that a suspended particle consists of an isotropic mixture of several components with known mass-specific coefficients of light absorption $a^*_i(\lambda)$ and known intraparticular concentrations C_i of these components (the subscript i here denotes the number or name of each component of the particle, i.e. a given substance or group of substances). Having made this assumption, we can now write the dependence of the coefficient of light absorption by particulate matter $a_{pm}(\lambda)$ and the imaginary refractive index of a particle $n'_p(\lambda)$ on the mass-specific absorption coefficients $a^*_i(\lambda)$ and the concentration C_i as follows:

$$a_{pm}(\lambda) = \Sigma_i a^*_i(\lambda) C_i, \tag{3a}$$

$$n'_p(\lambda) = \frac{\lambda}{4\pi} \Sigma_i a^*_i(\lambda) C_i. \tag{3b}$$

In line with our simplifying assumptions regarding the structure of POM, discussed in Part 1 (section 2 in Woźniak et al. 2005a), the general case of the model POM we are now analysing consists of three components: organic matter (OM), water (w), and air or some other gas (air). Given these assumptions, we can expand eqs. (3a) and (3b) to the following forms:

$$a_{pm}(\lambda) = a^*_w(\lambda) C_w + a^*_{\mathrm{OM}}(\lambda) C_{\mathrm{OM}} + a^*_{air}(\lambda) C_{air}, \tag{4a}$$

$$n'_p(\lambda) = \frac{\lambda}{4\pi} \left[a^*_w(\lambda) C_w + a^*_{\mathrm{OM}}(\lambda) C_{\mathrm{OM}} + a^*_{air}(\lambda) C_{air} \right], \tag{4b}$$

where a^*_w, a^*_{OM}, a^*_{air} are the respective mass-specific absorption coefficients of light in pure water, in pure organic material and in air (or other gas), and C_w, C_{OM}, C_{air} are the respective intraparticular concentrations of these three components.

Since both the physical and the optical densities of gases are negligibly small in comparison with the corresponding densities of organic matter and water, we can ignore the third terms in eqs. (4a) and (4b). Moreover, since the density of so-called neutral particles[6] (i.e. with zero buoyancy $b \approx 0$) is practically the same as that of the surrounding seawater ρ_w

[6]The division of suspended organic particles into three main physical types – neutral (or free), heavy and light particles – and numerous subtypes (e.g. neutral dry, neutral

(i.e. $C_w + C_{\mathrm{OM}} \approx \rho_w$), eqs. (4a) and (4b) can be reduced to operational formulas for determining the coefficients $a_{pm}(\lambda)$ and $n'_p(\lambda)$ of all the physical types and chemical classes of POM analysed in this paper on the basis of just three known magnitudes (or four in the general case – see eqs. (8a) and (8b)): (1) the coefficient of light absorption by water a_w, (2) the mass-specific absorption of organic matter a^*_{OM}, (3) the intraparticular concentration of this matter in a particle C_{OM}, and (4) the concentration of water in the particle C_w – in the general case. Hence, for particular types of particles, these formulas are the following:

– *free, dry particles* ($C_w = 0, C_{\mathrm{OM}} \approx \rho_w$, buoyancy $b \approx 0$):

$$a_{pm}(\lambda) = a^*_{\mathrm{OM}}(\lambda) C_{\mathrm{OM}}, \tag{5a}$$

$$n'_p(\lambda) = \frac{\lambda}{4\pi}\, a^*_{\mathrm{OM}}(\lambda) C_{\mathrm{OM}}; \tag{5b}$$

– *free, wet particles* ($C_w + C_{\mathrm{OM}} \approx \rho_w$, buoyancy $b \approx 0$):

$$a_{pm}(\lambda) = \frac{a_w(\lambda)}{\rho_w}(\rho_w - C_{\mathrm{OM}}) + a^*_{\mathrm{OM}}(\lambda) C_{\mathrm{OM}}, \tag{6a}$$

$$n'_p(\lambda) = \frac{\lambda}{4\pi}\left[\frac{a_w(\lambda)}{\rho_w}(\rho_w - C_{\mathrm{OM}}) + a^*_{\mathrm{OM}}(\lambda) C_{\mathrm{OM}}\right]; \tag{6b}$$

– *water particles (i.e. pure water)* ($C_w = \rho_w, C_{\mathrm{OM}} = 0$, buoyancy $b \approx 0$):

$$a_{pm}(\lambda) = a_w(\lambda), \tag{7a}$$

$$n'_p(\lambda) = \frac{\lambda}{4\pi}\, a_w(\lambda); \tag{7b}$$

– *heavy particles* ($C_w + C_{\mathrm{OM}} > \rho_w$, buoyancy $b < 0$) *and light particles* ($C_w + C_{\mathrm{OM}} < \rho_w$, buoyancy $b > 0$)[7]:

$$a_{pm}(\lambda) = \frac{a_w(\lambda)}{\rho_w} C_w + a^*_{\mathrm{OM}}(\lambda) C_{\mathrm{OM}}, \tag{8a}$$

$$n'_p(\lambda) = \frac{\lambda}{4\pi}\left[\frac{a_w(\lambda)}{\rho_w} C_w + a^*_{\mathrm{OM}}(\lambda) C_{\mathrm{OM}}\right]; \tag{8b}$$

– *heavy, pure organic particles* ($C_w = 0$, $C_{\mathrm{OM}} = \rho_{\mathrm{OM}} > \rho_w$, buoyancy $b < 0$):

$$a_{pm}(\lambda) = a^*_{\mathrm{OM}}(\lambda) \rho_{\mathrm{OM}}, \tag{9a}$$

$$n'_p(\lambda) = \frac{\lambda}{4\pi}\, a^*_{\mathrm{OM}}(\lambda) \rho_{\mathrm{OM}}, \tag{9b}$$

where ρ_{OM}, the density of dry organic matter, thus denotes the highest possible intraparticular concentration of organic matter in a particle, C_{OM}

wet, pure heavy, pure organic water particles, etc.) and some of the properties of these particles are discussed in Part 1 (see subsection 2.3 in Woźniak et al. 2005a).

[7]These eqs. (7a) and (7b) are also universal expressions, applicable to all physical types of model particles (i.e. to any value of C_w, C_{OM} and buoyancy b).

$\equiv \rho_{\mathrm{OM}}$. This concentration is characteristic of the heavy, pure organic particles under scrutiny here.

The above set of eqs. (5)–(9) is the algorithm for determining the resultant absorption properties (i.e. coefficients $a_{pm}(\lambda)$ and $n'_p(\lambda)$) of POM particles. In order to perform such calculations, we need to assume a number of physical magnitudes (the so-called model constants) and to state the input data. The model constants are ρ_w (density of pure water), ρ_{OM} (density of dry organic matter) and $a_w(\lambda)$ (the coefficients of light absorption by pure water for various wavelengths), while the input data comprises $a^*_{\mathrm{OM}}(\lambda)$ (spectral mass-specific coefficients of light absorption by the organic matter of a given POM particle), and C_{OM} and C_w (i.e. the average intraparticular concentrations of organic matter and water). Note that in the case of calculations for neutral (or free) particles (where $C_{\mathrm{OM}} + C_w = \rho_w$) and for pure organic particles (for which $C_w = 0$ and $C_{\mathrm{OM}} = \rho_{\mathrm{OM}}$), it is sufficient to know just the intraparticular organic matter concentration C_{OM}.

3.2. The model constants

The following values or sets of values of the above-mentioned physical parameters were assumed for the model constants:

- the density of pure sea water ρ_w was assumed, for the sake of simplicity, to take a value of 10^3 kg m^{-3} under normal conditions;
- again, for simplicity's sake, the density of dry organic matter ρ_{OM} was set equal for the organic matter in all 26 model chemical classes of POM: $\rho_{\mathrm{OM}} = 1.4 \times 10^3$ kg m^{-3} (after Woźniak et al. 2005a); this value approaches the densities of the pure forms of proteins and carbohydrates[8]: 1335 kg m^{-3} and 1530 kg m^{-3} respectively (after Morel & Ahn 1990);
- the spectral coefficients of light attenuation by pure water $a^*_w(\lambda)$ for various wavelengths λ in the spectral range 200–700 nm, were taken from various papers (Smith & Baker 1981, Pope & Fry 1997, Sogandares & Fry 1997); they are given in Table 3.

3.3. The input data

Since the calculations covered all 26 chemical classes of POM, the input data of $a^*_{\mathrm{OM}}(\lambda)$ included 26 sets of spectra of the mass-specific coefficients

[8]In actual fact, the densities of pure organic substances (except organic gases) under normal conditions can vary, from slightly less than the density of water to values exceeding this density by over 50%. However, most of the compounds naturally occurring in organisms are or resemble proteins or carbohydrates.

Table 3. Spectral absorption coefficients of the water used in this paper*

Light wavelength [nm]	a_w [m^{-1}]	Light wavelength [nm]	a_w [m^{-1}]	Light wavelength [nm]	a_w [m^{-1}]
200	3.07	370	0.0114	540	0.0474
205	2.53	375	0.011385	545	0.0511
210	1.99	380	0.01137	550	0.0565
215	1.65	385	0.00941	555	0.0596
220	1.31	390	0.00851	560	0.0619
225	1.1185	395	0.00813	565	0.0642
230	0.927	400	0.00663	570	0.0695
235	0.8235	405	0.0053	575	0.0772
240	0.72	410	0.00473	580	0.0896
245	0.6395	415	0.00444	585	0.11
250	0.559	420	0.00454	590	0.1351
255	0.508	425	0.00478	595	0.1672
260	0.457	430	0.00495	600	0.2224
265	0.415	435	0.0053	605	0.2577
270	0.373	440	0.00635	610	0.2644
275	0.3305	445	0.00751	615	0.2678
280	0.288	450	0.00922	620	0.2755
285	0.2515	455	0.00962	625	0.2834
290	0.215	460	0.00979	630	0.2916
295	0.178	465	0.01011	635	0.3012
300	0.141	470	0.0106	640	0.3108
305	0.123	475	0.0114	645	0.325
310	0.105	480	0.0127	650	0.34
315	0.0947	485	0.0136	655	0.371
320	0.0844	490	0.015	660	0.41
325	0.0761	495	0.0173	665	0.429
330	0.0678	500	0.0204	670	0.439
335	0.06195	505	0.0256	675	0.448
340	0.0325	510	0.0325	680	0.465
345	0.02645	515	0.0396	685	0.486
350	0.0204	520	0.0409	690	0.516
355	0.018	525	0.0417	695	0.559
360	0.0156	530	0.0434	700	0.624
365	0.0135	535	0.0452		

* values assumed on the basis of data from various authors and linear approximation: in the range 200–335 nm after Smith & Baker 1981, 340–370 nm after Sogandares & Fry 1997, 380–700 nm after Pope & Fry 1997.

of light absorption by POM, as described in section 2 (see Tables 1 and 2, and Fig. 1).

However, the intraparticular concentrations of organic matter C_{OM} (and possibly of interstitial water) depended on the physical type of particle, or particles with properties similar to a given type:

- *neutral (free) dry particles and similar particles*, i.e. particles of organic matter with a resultant mean density approaching that of the surrounding seawater, not containing any interstitial water, but with spaces that could be filled with air or some other gas, thereby attaining zero (or almost zero) buoyancy. For such particles, it was assumed that $C_{\mathrm{OM}} = 1000$ kg m^{-3} and $(C_w = 0)$;
- *neutral (free) wet particles and similar particles*, i.e. particles of organic matter also with a resultant mean density similar to that of the surrounding seawater, but differing from dry particles in that they additionally contain water-filled interstices, and together with this water and air attain zero (or almost zero) buoyancy. Theoretically, this water content can range from 0% to 100%; in the extreme cases, such a particle becomes a water particle (100% water content) or a free, dry particle (0% water content). In this paper we present the results of calculations done for particles with a 90% water content, i.e. for which $C_{\mathrm{OM}} = 100$ kg m^{-3} ($C_w = 900$ kg m^{-3});
- *pure heavy particles (purely organic particles) and similar particles*, that is, with densities greater than that of the surrounding water and containing solely organic matter, i.e. without any air- or water-filled interstices. These particles have a decidedly negative buoyancy, so in the absence of other forces in the water acting on them (a condition not normally satisfied in the sea), they sink freely. The concentration of organic matter in these particles was thus assumed to be equal to the density of the dry organic matter: $C_{\mathrm{OM}} = \rho_{\mathrm{OM}} = 1400$ kg m^{-3} and $(C_w = 0)$;
- *virtual water particles*, in other words, pure water: $C_{\mathrm{OM}} = 0$ ($C_w = \rho_w = 1000$ kg m^{-3}). Formally, this case can be classified among the neutral (free) wet particles.

Restricting the analysis to these few physical types of particles is justified by the fact that they are the ones most commonly appearing and remaining in the water (see the reasoning given in Part 1, subsection 2.3 (Woźniak et al. 2005a)). Dry particles and particles with an average water content, i.e. particles with a water content less than or equal to 90% of the particle volume (for $C_{\mathrm{OM}} \geq 100$ kg m^{-3}) are most likely to occur in the water. We shall return in subsection 4.3 to this conventional division into moderately and strongly hydrated particles.

These physical types of particles also cover extreme cases: on the one hand, the pure organic particles and the neutral dry organic particles, and on the other, the pure water particles. The results of the following analysis thus characterise the possible range of variation in the absorption properties of organic particles, which is thus applicable to practically all types of POM particles, and not just to the most numerous ones.

4. The imaginary refractive index of different chemical classes and physical types of POM

Our calculations yielded a set of 79 model spectra of the imaginary part of the absolute refractive index $n'_p(\lambda)$ for the various types of POM. To this end we used the algorithm described in section 3, the data on mass-specific light absorption coefficients for POM described in section 2, and the other input data described in section 3. The calculated spectra of $n'_p(\lambda)$ respectively represent all 26 chemical classes of POM and three physical types of particles characteristic of the POM most commonly occurring in sea water (this includes the spectra of $n'_w(\lambda)$ for 'water particles', i.e. for pure water). Some of the results are presented in Table 4, but all the calculated spectra are illustrated in Fig. 2, panels (a) to (l). For the purposes of comparison, all the graphs include the spectrum of $n'_{p,SS}(\lambda)$ for Sargasso Sea detritus, determined by Stramski et al. (2001) on the basis of empirical data obtained by Iturriaga & Siegel (1989).

As can be seen from the graphs (Fig. 2), the model spectra of $n'_p(\lambda)$ for the various chemical classes and physical types of POM are highly diverse, both with respect to their spectral structure and to the absolute values of n'_p. This section analyses and discusses the spectral characteristics of $n'_p(\lambda)$ (subsection 4.1), then the variability in the absolute values of these indices (subsection 4.2); finally, the ranges of n'_p possible to occur in natural waters are estimated (subsection 4.3).

4.1. Analysis of the spectral differentiation of $n'_p(\lambda)$

The model chemical classes of particles containing a single organic component exhibit the most distinctive and selective features of the spectra of $n'_p(\lambda)$ (see Figs 1a, 1b, 1c). This applies in particular to particles of *classes A1*, *A2* and *N*, that is, to those containing the most homogeneous organic matter, consisting of strongly UV-absorbing compounds:

– *class A1* particles (aromatic amino acids), with two strong absorption bands in the $n'_p(\lambda)$ spectrum in the c. 200–220 nm and 280 nm regions;

– *class N* particles (purine and pyridine compounds containing adenine, guanine and cytosine) with strong absorption in the c. 220 nm and c. 260 nm regions;

– *class A2* particles (mycosporine-like amino acids – MAAs), with very strong absorption bands in the $n'_p(\lambda)$ spectrum in the 300–365 nm region.

Particles from these three classes absorb light in the UV, usually the far-UV, spectral regions. Any absorption of light (n'_p) outside these regions can be neglected. These properties are mainly the result of well-defined $\pi \rightarrow \pi^*$ energy transitions, i.e. conjugated π-electrons belonging to the aromatic ring (in the case of aromatic amino acids – *class A1*), or to such rings conjugated with various hyperchromic auxochromes, which leads to bathochromic shifts in the absorption bands (in the case of MAAs, i.e. *class A2*), or to purine and pyridine rings containing nitrogen atoms (*class N*) (see e.g. Campbell & Dwek 1984, Kęcki 1993).

Somewhat less well defined, but nevertheless with a distinct band structure in the UV region, is the spectrum of $n'_p(\lambda)$ for *class L*, the particles containing lignins. Chemically, lignins are complex products of the biosynthesis of carbohydrates and aromatic amino acids (phenylalanine and tyrosine) and form rigid, three-dimensional polymeric structures cementing the cellulose fibres of higher plants together (Meyers-Schulte & Hedges 1986). Owing to the great similarity in chemical structures between lignins and aromatic amino acids, the absorption properties of the former in the 200–300 nm region are also similar to those of the latter. We thus see a distinct light absorption maximum in the vicinity of wavelengths $\lambda \approx 250$ nm. But unlike the aromatic amino acids, lignins also absorb radiation longer than 300 nm quite strongly. This is due to the greater diversity of auxochromic substituents in the benzene ring in their structure, and also to possible conjugations between the separate aromatic rings in their polymeric structure.

The band structure of $n'_p(\lambda)$ spectra is also distinctive in the chemical *classes P1* (oceanic phytoplankton pigments) and *P2* (Baltic phytoplankton pigments), which contain VIS absorbers: there are two well-known, quite broad absorption bands (in fact comprised of a series of narrower bands due to the component pigments) around 440 nm (the Soret band) and in the region around 675 nm. As we know, these absorption bands are also generated by energy transitions of the conjugated π-electrons in the long, mainly linear polymer chains of carotenoid pigments, in the five double-bond-rich piryl rings enveloped in the porphyrin structure of chlorophyll pigments, or in the open tetrapiryl chain of the various phycobilins (see e.g. Shlyk (ed.) 1974, Scheer 1991, Jeffrey et al. 1997, Majchrowski 2001).

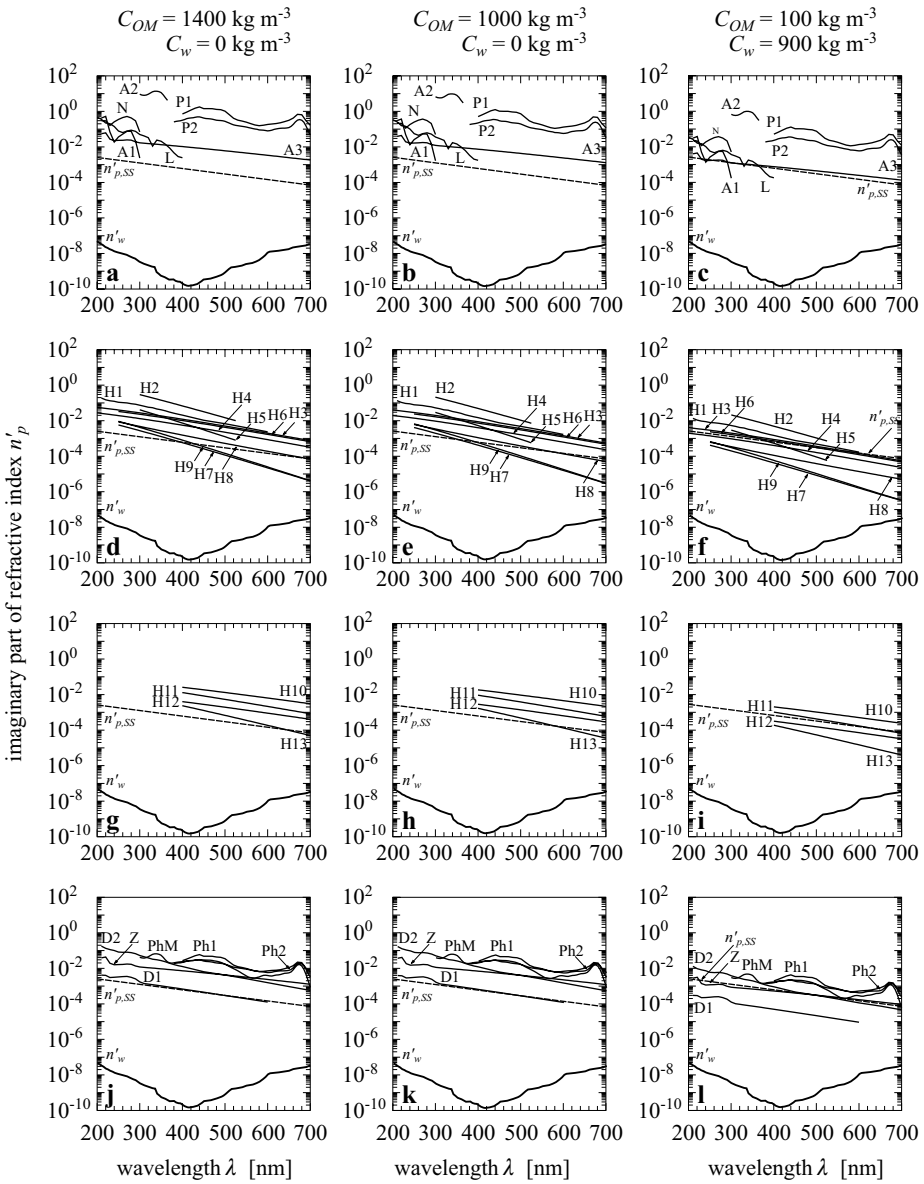

Fig. 2. Spectra of the imaginary refractive index for the model POM from various chemical classes: (a), (b), (c) single-component organic particles; (d), (e), (f) particles containing organic humus matter originating from different marine basins; (g), (h), (i) particles containing organic humus matter produced in the soil and bottom sediments; (j), (k), (l) multi-component organic particles; and belonging to different physical types: (a), (d), (g), (j) pure organic particles (C_{OM} = 1400 kg m^{-3}, C_w = 0); (b), (e), (h), (k) neutral dry particles (C_{OM} = 1000 kg m^{-3}, C_w = 0); (c), (f), (i), (l) neutral wet particles (C_{OM} = 100 kg m^{-3}, C_w = 900 kg m^{-3}); The solid line (*continued next page*)

in the graphs illustrates the spectrum of the absolute imaginary refractive index of water $n'_w(\lambda)$ (or in a particle composed exclusively of water). The dashed line represents the spectrum of $n'_{p,ss}(\lambda)$ for Sargasso Sea detritus (after Stramski et al. 2001). The graphs for the model particles were drawn on the basis of the data and equations given in Tables 1, 2 and 3

Of the model chemical classes of particles containing one organic component, the least selective are the $n'_p(\lambda)$ spectra for *class A3*, i.e. particles consisting of natural proteins or their fragments (peptides). As we can see from Fig. 2 (a, b, c) (see curve A3), there are two distinct absorption bands in this spectrum, in the regions around 220 nm and 280 nm, characteristic of all proteins, which are due to the aromatic amino acids present in them (cf. curves A1 and A3 on Fig. 2 (a, b, c)). But unlike the latter, proteins also absorb quite strongly in all regions of the UV and VIS. This is due to the wide range of various substructures (all other amino acids and submolecular admixtures in proteids) present in naturally occurring molecules, which turn out to be chromophoric groups. Hence, natural proteins absorb light in various regions of the UV-VIS spectrum. Note, however, that this absorption decreases monotonically with increasing wavelength, and that this fall is described by an exponentially diminishing curve (see eq. (T1) in Table 1a). But in reality, the $n'_p(\lambda)$ spectra for separate proteins are not as 'smooth' as the approximate model description, statistically averaged over a range of proteins, would have us believe. Such real spectra can display a whole series of separate, strong absorption bands in different spectral regions (see Fig. A.2.1d in Appendix 2), but different for various forms of proteins.

Apart from single-component particles, those from chemical classes that we have classified among the multi-component particles of organic matter can exhibit an often considerable spectral selectivity with regard to absorption (see Figs 2j, 2k and 2l). This is reasonable, since particles from this group are often simply mixtures of substances consisting of single-component organic matter. That is why the same absorption bands appear in their $n'_p(\lambda)$ spectra as in the case of single-component particles. There may well be an even greater number of these bands, but they will be less distinct.

The structure of the $n'_p(\lambda)$ spectra of humus particles is the least distinct, no matter whether they originated in water, soils or bottom sediments – see Figs 2d, e, f and Figs 2g, h, i. These figures show that humus particles strongly absorb both UV and VIS radiation, although the absorption coefficient falling monotonically with increasing wavelength is a feature of all

Table 4. The imaginary part of the absolute refractive index of UV-VIS light of selected wavelengths for (1) 26 model chemical classes of POM occurring in the form of pure organic particles $n'_{p,dry}$ and (2) 'water particles' n'_w

Particle	Imaginary part of the refractive index n' for wavelength λ [nm]						
class	200	230	280	300	340	400	420
A1	–	6.92E–02	7.49E–02	2.34E–03	(0)	(0)	(0)
A2	–	–	–	9.26E+00	1.36E+01	–	(0)
A3	–	2.73E–02	2.39E–02	1.70E–02	1.40E–02	1.04E–02	9.37E–03
P1	(0)	(0)	(0)	(0)	–	7.13E–01	1.18E+00
P2	(0)	(0)	(0)	(0)	–	3.16E–01	4.30E–01
N	–	1.61E–01	4.27E–01	7.02E–02	(0)	(0)	(0)
L	4.72E–01	2.02E–01	8.73E–02	5.01E–02	2.42E–02	2.45E–03	(0)
H1	–	1.31E–01	9.05E–02	7.35E–02	4.55E–02	2.05E–02	1.64E–02
H2	–	–	–	2.92E–01	1.65E–01	6.77E–02	5.01E–02
H3	5.56E–02	4.58E–02	3.20E–02	2.75E–02	2.00E–02	1.21E–02	1.02E–02
H4	2.72E–02	2.22E–02	1.53E–02	1.31E–02	9.38E–03	5.57E–03	4.66E–03
H5	–	–	–	4.07E–02	2.08E–02	7.35E–03	5.18E–03
H6	–	–	2.66E–02	2.29E–02	1.67E–02	1.02E–02	8.56E–03
H7	–	–	3.69E–03	2.74E–03	1.49E–03	5.79E–04	4.21E–04
H8	–	–	5.98E–03	4.75E–03	3.01E–03	1.54E–03	1.24E–03
H9	–	–	5.76E–03	4.19E–03	2.18E–03	8.02E–04	5.71E–04
H10	–	–	–	–	–	2.58E–02	2.27E–02
H11	–	–	–	–	–	1.29E–02	1.09E–02
H12	–	–	–	–	–	4.01E–03	3.48E–03
H13	–	–	–	–	–	2.36E–03	1.85E–03
Ph1	–	*1.87E–02*	*1.70E–02*	*8.50E–03*	*7.00E–03*	2.70E–02	4.10E–02
Ph2	–	*1.87E–02*	*1.70E–02*	*8.50E–03*	*7.00E–03*	2.14E–02	2.70E–02
Z	–	1.91E–02	1.67E–02	1.19E–02	9.81E–03	7.28E–03	6.56E–03
D1	–	3.04E–03	3.10E–03	1.72E–03	1.11E–03	6.82E–04	5.77E–04
D2	–	1.14E–01	7.59E–02	5.22E–02	3.05E–02	1.25E–02	1.00E–02
PhM	–	*1.87E–02*	*1.70E–02*	4.17E–02	6.52E–02	2.35E–02	2.73E–02
n'_w	4.89E–08	1.70E–08	6.42E–09	3.37E–09	8.79E–10	2.11E–10	1.52E–10

	Imaginary part of the refractive index n' for wavelength λ [nm]						
	440	500	550	600	650	675	700
A1	(0)	(0)	(0)	(0)	(0)	(0)	(0)
A2	(0)	(0)	(0)	(0)	(0)	(0)	(0)
A3	8.42E–03	6.03E–03	4.52E–03	3.36E–03	2.48E–03	2.12E–03	1.82E–03
P1	1.77E+00	1.03E+00	2.45E–01	1.83E–01	3.15E–01	7.01E–01	1.66E–01
P2	4.88E–01	2.74E–01	1.31E–01	8.00E–02	1.23E–01	3.45E-01	4.66E–02
N	(0)	(0)	(0)	(0)	(0)	(0)	(0)
L	(0)	(0)	(0)	(0)	(0)	(0)	(0)
H1	1.31E–02	6.68E–03	4.04E–03	2.34E–03	–	–	–
H2	3.70E–02	1.47E–02	–	–	–	–	–
H3	8.52E–03	4.97E–03	3.14E–03	1.97E–03	1.22E–03	9.63E–04	7.56E–04
H4	3.88E–03	2.23E–03	1.39E–03	8.55E–04	5.24E–04	4.09E–04	3.19E–04
H5	3.63E–03	1.24E–03	–	–	–	–	–
H6	7.20E–03	4.23E–03	2.68E–03	1.69E–03	1.06E–03	8.33E–04	6.56E–04
H7	3.05E–04	1.15E–04	5.04E–05	2.19E–05	9.46E–06	6.20E–06	4.06E–06
H8	9.95E–04	5.26E–04	3.14E–04	1.89E–04	1.14E–04	8.88E–05	6.92E–05

Table 4. (*continued*)

Particle class	Imaginary part of the refractive index n' for wavelength λ [nm]						
	440	500	550	600	650	675	700
H9	4.06E–04	1.44E–04	6.01E–05	2.48E–05	1.02E–05	6.52E–06	4.17E–06
H10	1.98E–02	1.31E–02	9.21E–03	6.41E–03	4.43E–03	3.67E–03	3.04E–03
H11	9.16E–03	5.38E–03	3.41E–03	2.15E–03	1.34E–03	1.06E–03	8.34E–04
H12	3.02E–03	1.94E–03	1.33E–03	9.00E–04	6.06E–04	4.96E–04	4.06E–04
H13	1.44E–03	6.75E–04	3.55E–04	1.85E–04	9.61E–05	4.77E–04	4.95E–05
Ph1	5.88E–02	3.47E–02	9.72E–03	7.26E–03	1.09E–02	2.50E–02	6.00E–03
Ph2	2.96E–02	1.72E–02	8.99E–03	5.74E–03	7.63E–03	1.93E–02	3.28E–03
Z	5.89E–03	4.22E–03	3.16E–03	2.35E–03	1.73E–03	1.49E–03	1.27E–03
D1	4.88E–04	2.95E–04	1.93E–04	1.26E–04	–	–	–
D2	8.05E–03	4.16E–03	2.59E–03	1.56E–03	9.37E–04	7.29E–04	5.68E–04
PhM	3.08E–02	1.70E–02	3.73E–03	3.96E–03	5.53E–03	1.65E–02	8.46E–04
n'_w	2.22E–10	8.12E–10	2.47E–09	1.06E–08	1.76E–08	2.41E–08	3.48E–08

Explanations: (–) – the values of the index n'$_p$ were not defined; 0 – the values of the index n'$_p$ are much smaller than in other spectral intervals; extrapolated values are given in italics.

these spectra. There are hardly any local maxima[9]. Moreover, these spectra are almost exactly exponential. The smoothness of the $n'_p(\lambda)$ spectra of light absorption by humus particles is due to the enormous complexity of their chemical structures and the presence in them of a huge number of different chromophoric groups absorbing radiation in almost all UV-VIS regions.

4.2. Analysis of the diversity in absolute values of indices n'_p

Another feature characterising the model spectra of the imaginary refractive index $n'_p(\lambda)$ of the various chemical classes and physical types of particles is the extremely wide variation in the absolute values of n'_p, covering many orders of magnitude (see Fig. 2). This diversity is easily explained and described with respect to the indices $n'_p(\lambda)$ for the various physical types of particles from the same chemical classes. The highest values of these imaginary refractive indices (Table 4; Fig. 2, left-hand column of graphs – a, d, g, j) apply to those chemical classes of particles that exist in the form of pure organic matter (which corresponds to the physical type 'pure organic or pure heavy particles'), that is, to an intraparticular concentration of organic matter equal to the density of the dry organic

[9]Exceptional are some particles consisting of humus from bottom sediments, or humus produced in organic detritus (but not from organic matter dissolved in the water). In their spectra (e.g. in the region of the wavelengths : 440, 460–470, 665–675 nm), we sometimes see bulges or inflexion points, which are caused by the presence of plant pigment fragments in these compounds (Pempkowiak 1989).

matter, which in this work is assumed to take the average value of $C_{\mathrm{OM}} = \rho_{\mathrm{OM}} = 1400$ kg m^{-3}. For all the other physical types, the values of n'_p diminish with falling concentration C_{OM} (compare the left-hand, middle and right-hand columns of the graphs on Fig. 2 with one another). In the limiting case, when $C_{\mathrm{OM}} \approx 0$, the index $n'_p(\lambda)$ takes the value for pure water[10] i.e. $n'_p(\lambda) \approx n'_w(\lambda)$.

It is also worth drawing attention to the fact that for the most commonly occurring physical types of particles in the water, i.e. neutral wet particles and such like, and also for heavy particles containing water, $n'_p(\lambda)$ takes values that are almost directly proportional to their organic matter content C_{OM} and does not exhibit any visible dependence on the absorption properties of water, even though such a dependence formally exists (see e.g. eqs. (5b) and (7b)). As we showed in Part 1 (subsection 3.2 in Woźniak et al. 2005a), this can be explained by the fact that very much more light is absorbed by even tiny quantities of organic matter than by water. This is because the mass-specific absorption coefficients of UV-VIS light for water are many orders of magnitude smaller than for the organic substances we are analysing here. Light absorption by the water contained in particles will therefore exceed that by the particles themselves only when the organic matter content is extremely low ($C_{\mathrm{OM}}/C_w \approx 10^{-7}$ and less).

An important practical conclusion can be drawn from the above. It is that the spectral values of the imaginary refractive indices $n'_{p,dry}$ set out in Table 4 for all 26 chemical classes of particles containing pure organic matter can also be used to determine the imaginary refractive indices n'_p for practically all physical types of particles that commonly occur in the sea. So, if we know the intraparticular concentration of organic matter C_{OM}, we can calculate the refractive indices for the various physical types of particles from the following approximate relationship:

$$n'_p \approx n'_{p,dry} \frac{C_{\mathrm{OM}}}{\rho_{\mathrm{OM}}}, \tag{10}$$

where $n'_{\mathrm{p,dry}}$ and n'_p are the respective imaginary refractive indices for particles containing dry organic matter (data in Table 4) and for particles with any intraparticular concentration of organic matter C_{OM}; ρ_{OM} is the density of dry organic matter assumed in this model ($\rho_{\mathrm{OM}} = 1400$ kg m^{-3}).

[10]Theoretically, it is also possible for $n'_p(\lambda)$ to be smaller than $n'_w(\lambda)$ (see the analysis of this problem in Part 1, subsection 3.2 in Woźniak et al. 2005a). This happens in the case of the highly unlikely, extremely light three-component particles (organic matter, water and gas), or two-component particles (only organic matter and gas), further containing exceedingly low levels of organic matter (of the order of 10^{-4} kg m^{-3} and less). Such particles can hardly be treated as POM; rather, they are air bubbles.

The second factor governing the absolute values of the imaginary refractive indices for POM (besides the intraparticular concentration of organic matter C_{OM}) are the types and compositions of the various organic substances contained in the particles. The values of n'_p are determined by the individual absorption capacities of all the organic components in the particle. On the other hand, they are directly dependent on the resultant mass-specific coefficients of light absorption $a^*_{\mathrm{OM}}(\lambda)$ (see Fig. 1) for all these mixtures of compounds, no matter whether they are strong or weak absorbers of light. That is why the values of n'_p for the 26 model chemical classes of particles (differing fundamentally in their proportions of strongly or weakly absorbing, or non-absorbing, organic components) vary over several orders of magnitude (see the graphs on the different levels of the panels in Fig. 2).

Thus, the highest values of n'_p are characteristic of the chemical classes of single-component organic particles (see Figs 2a, b, c): these are assumed to consist only of the strongest UV and/or VIS absorbers among naturally occurring organic compounds, without any admixture of weak absorbers. Far lower values of n'_p (by around 2 to 3 orders of magnitude in certain spectral intervals) are typical of particles consisting of organic humus matter (compare the graphs in Figs 2a, b, c with those in Figs 2d, e, f and Figs 2g, h, i). By their very nature, humus substances have much lower mass-specific coefficients of light absorption than, say, pigments (*classes P1* and *P2*) in the VIS region, or various amino acids and purine and pyridine compounds (*classes A1*, *A2*, *N*) in the UV region[11] – see Figs 1a, b, c.

The imaginary refractive indices n'_p of multi-component particles of organic matter in certain spectral regions are lower by 1 to 2 orders of magnitude in comparison with the values of n'_p for single-component particles (see the graphs in Figs 2a, b, c and j, k, l). This is because, apart from strong absorbers like the compounds in single-component particles, multi-component particles contain considerable quantities of humus substances, which absorb light less strongly, and also organic matter that absorbs hardly any light in the UV-VIS intervals we are interested in.

Of course, POM in the sea may also contain particles consisting solely or mostly of organic matter absorbing light very weakly or with even lower values of n'_p than described above. In all probability, however, the percentage of such particles is quite low.

[11]However, humus substances do absorb both UV and VIS radiation. Their refractive indices are thus much higher than those for *classes A1*, *A2* and *N* in the VIS region and for *classes P1* and *P2* in the UV region.

4.3. Estimating the possible range of the imaginary refractive index n'_p in natural waters

Our calculations of the imaginary refractive index n'_p for the various chemical classes and physical types of POM have enabled a preliminary estimate of its probable range of variability in the World Ocean to be made, with respect not only to POM in general, but also to the various chemical classes of these particles.

The complex graph of the dependence of n'_p on the light wavelength (Fig. 3) gives a good idea of the nature of the problem. When constructing this graph, we selected a number of model spectra of $n'_p(\lambda)$ from our set of spectra determined for different physical types and chemical classes of POM (including extremely high ones), as well as the spectrum of $n'_w(\lambda)$ for 'water particles' (i.e. for pure water). Moreover, taking into account the various possible physical types of POM, we decided to divide these into two groups[12]:

a) *strongly hydrated particles*, with a water content in excess of 90% by volume (i.e. an organic matter concentration $C_{\mathrm{OM}} < 100$ kg m^{-3}); these are probably very rarely found in the water;

b) *dry or moderately hydrated* particles, with a water content less than or equal to 90% by volume (i.e. an organic matter concentration $C_{\mathrm{OM}} \geq 100$ kg m^{-3}); such particles are probably common in the water.

Having made these assumptions and using the envelope method, we determined a number of conventional value areas of the imaginary refractive index for POM n'_p on the plot of n'_p vs λ (Fig. 3), corresponding to various ranges of variability of their absolute magnitudes. The most important of these, shown on Fig. 3, are:

1) the *range of variability of n'_p for all particles* (i.e. regardless of their frequency of occurrence) – see area I in Fig. 3;

[12]In assuming this boundary (90% water content and $C_{\mathrm{OM}} = 100$ kg m^{-3}) separating the strongly hydrated particles (probably rare) from the moderately hydrated or dry ones (common), we took our yardstick to be the biochemical composition of marine organisms – see Table A4.1 in Appendix 4. We further assumed that in water we most frequently come across particles with water and organic matter contents that are roughly the same as those in living organisms, because they either are such organisms (plankton cells) or are the partially or completely dehydrated remains of organisms, their discrete organelles, and faeces, that is with a lower water content and a higher organic matter content (also in the pure form). This division is therefore justified with respect to many chemical classes of single- and multi-component organic particles or fragments of phytoplankton, zooplankton and nekton. But with respect to all humus particles and particles of *classes D1* and *D2*, for example, this division is far more symbolic.

2) the *range of variability of* n'_p *for dry and moderately hydrated single- and multi-component particles*, commonly occurring in the water – see area II in Fig. 3;

3) *range of variability of* n'_p *for dry and moderately hydrated humus particles* – see area III in Fig. 3.

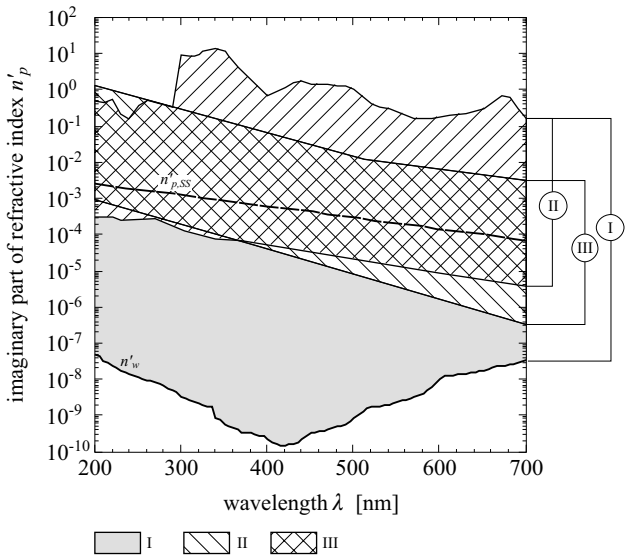

Fig. 3. The probable ranges of differentiation in the spectra of the imaginary refractive index $n'_p(\lambda)$ for: area I – all POM particles; area II – dry or moderately hydrated, single-component and multi-component particles of organic matter; area III – dry and partially hydrated particles consisting of marine or soil/bottom-sediment humus (see explanations in the text)

The upper boundary of area I, illustrating the range of variability of n'_p for all particles, is the upper envelope covering the spectra of $n'_p(\lambda)$ with the highest values of n'_p for the chemical classes of single-component organic particles (in particular *A1*, *N*, *A2* and *P1* – see Fig. 2a), occurring in the form of pure organic particles (i.e. $C_{\mathrm{OM}} = 1400$ kg m^{-3}). Beyond the lower boundary of this area we assume (as we stated in subsection 4.2) the spectrum of $n'_w(\lambda)$ for pure water. The position of area I on the graph implies that the probable diversity of n'_p for any POM particles is vast, and may, depending on the light wavelength, extend over more than a dozen orders of magnitude. The highest value of this index, modelled for dry organic matter in *class A2* particles (MAAs) in the spectral region c. 340 nm is around $n'_p = 13.6$, and is almost 10^{11} times greater than the smallest value of this index $n'_w = 1.52 \times 10^{-10}$, characteristic of water particles in the

spectral region c. 420 nm. The diversity of these indices is somewhat less for identical light wavelengths: c. 8–10 orders of magnitude for UV radiation, and 9 orders of magnitude at c. 400 nm and c. 7 orders of magnitude at c. 700 nm for VIS radiation.

This range of diversity of indices n'_p under natural conditions, i.e. with respect to the most common marine POM, is probably smaller. The suspended matter probably most frequently present in the water consists of moderately hydrated or dry single- and multi-component particles of organic matter[13]. The range of diversity of indices n'_p we have modelled for such particles is outlined by area II in Fig. 3. For obvious reasons, the upper boundary of this area is the same as for all particles (i.e. as for area I). But its lower boundary is the lower envelope of the set of spectra of $n'_p(\lambda)$ calculated for 90% hydrated multi-component particles (i.e. $C_{\mathrm{OM}} = 100$ kg m^{-3}), which in this case overlaps curve D1 in Fig. 2l. The position of area II on the graph (Fig. 3) implies that the range of variability of n'_p for dry and slightly hydrated single- and multi-component organic particles, probably common in the sea, is roughly the same for different wavelengths and covers 4 to 6 orders of magnitude.

It is likely that dry and moderately hydrated humus particles are also quite common in the sea. The possible range of variability of n'_p for such particles is given by area III in Fig. 3. Its upper boundary is given by the upper envelope of the spectrum of $n'_p(\lambda)$ in Fig. 2b (mainly overlapping the spectrum of $n'_p(\lambda)$ for dry humus of *class H2*), whereas the lower boundary overlaps the spectrum of $n'_p(\lambda)$ for *class H7* particles (see Fig. 2f) with an intraparticular organic matter content of $C_{\mathrm{OM}} = 100$ kg m^{-3}. We see that the area of variability of $n'_p(\lambda)$ for humus particles on the n'_p vs λ plot is somewhat narrower than in area II and usually lies in the lower part of area II, extending over three to four orders of magnitude.

To end with, let us have a look at one of the few existing empirical spectra of the imaginary refractive index $n'_{p,SS}(\lambda)$, already illustrated in Figs. 2 and 3 for the purposes of comparison. Stramski et al. (2001) determined it from microspectrophotometric measurements in the Sargasso Sea (Iturriaga & Siegel 1989) in order to complement their multi-component model of the inherent optical properties of the ocean. In their modelling efforts they emphasised the influence of changes in living planktonic community composition on optical properties of seawater. They took into account 18 different living planktonic components (viruses,

[13]The problems concerning the chemical compositions and physical types of the various morphological types of POM actually present in the sea are currently being addressed. We hope to return to them in Part 3 of this cycle of articles.

heterotrophic bacteria and microplanktonic species). To complement that model, Stramski and his collaborators also took three simplified classes representing non-living particles suspended in seawater: organic detritus (described by the above-mentioned spectrum of $n'_{p,SS}(\lambda)$, mineral particles and air bubbles. Their results generally demonstrated that multi-component approach to describing the living fraction of POM promised significant improvements in our understanding of seawater optics. The results of our own studies, here illustrated in Fig. 3 and earlier in Fig. 2, show that future multi-component optical models can and should be extended by also taking into account several possible types of non-living POM with diverse values of $n'_p(\lambda)$.

5. Conclusions

The objectives of this work, covering the second stage of modelling and the first results of the light absorption properties of particulate matter forming organic particles suspended in sea water, have been achieved. The light absorption capacities, or more precisely, the spectra of the mass-specific absorption coefficients $a^*_{\mathrm{OM}}(\lambda)$ were established for 26 naturally occurring organic substances or their possible mixtures, capable of forming particulate organic matter (POM) in the sea (see Tables 1 and 2, and Fig. 1). This was done by reviewing and then averaging a whole range of literature data, and by applying the results of our own theoretical and empirical research. The set of model spectra of $a^*_{\mathrm{OM}}(\lambda)$ obtained in this way were used to model spectra of the resultant absorption properties of POM, such as the absorption coefficients of particulate matter (both organic and inorganic) $a_{pm}(\lambda)$, and the imaginary parts of the complex refractive index of light for particulate matter $n'_p(\lambda)$. This set of 26 spectra of the mass-specific absorption coefficients $a^*_{\mathrm{OM}}(\lambda)$ appears to be an original approach to solving this complex question: it is the first systematic and synthesised set of light absorption capacities for a whole range of organic matter forms occurring naturally in the sea.

A suitable algorithm was constructed and with the aid of the set of spectra $a^*_{\mathrm{OM}}(\lambda)$ was used to determine the spectra of the imaginary refractive index $n'_p(\lambda)$ characteristic of the various chemical classes and physical types of POM commonly occurring in the sea (Fig. 2). This enabled the probable ranges of variability of n'_p to be estimated quantitatively for all POM in the sea and for certain groups of these suspended particles (see Fig. 3).

The results of these analyses led to a practical conclusion, significant as regards modelling the resultant inherent optical properties of sea water (absorption coefficients in particular), among other things, on the basis of known imaginary refractive indices of suspended particles $n'_p(\lambda)$. In view of

the enormous range of variability of n'_p demonstrated for various POM in the sea, such modelling will have to take a multi-component approach and make allowance for the existence of many POM components with different values of n'_p, with respect to both the living and the non-living fractions of this POM. Taking this multi-component approach only with respect to the plankton (i.e. the living fractions of POM) does not appear to be sufficient.

One shortcoming of the model spectra of $n'_p(\lambda)$ presented here concerns our assumption of the hypothetical (excluding the phyto- and zooplankton) groups of POM in the sea. These are groups of particles whose existence has not yet been empirically verified. In our view, these results present just a preliminary picture of the spectral variety of $n'_p(\lambda)$, yet it appears to be a correct one. The probable natural range of variability of this index for marine POM seems equally correct. Nevertheless, these results are not yet sufficient to set up a model data base of spectra of $n'_p(\lambda)$ for the non-living fractions of POM, which could be put to use in any future multi-component modelling of the resultant inherent optical properties of the sea with the requisite accuracy.

In order to eliminate these inadequacies from the modelling of n'_p for marine POM, the hypothetical chemical classes and physical types of POM we have been dealing with at the present stage of our research will have to be firmly linked to real morphological types of suspended matter. Only then will we be able to characterise the light absorption properties (including the index n'_p) of these real morphological types. Our current studies are focused on precisely these problems, and we hope to be able to present the results in *Oceanologia* in Part 3 of this cycle of articles.

Acknowledgements

Our grateful thanks go to Dr T. A. Moisan for her kindness in making available to us her invaluable empirical data on the light absorption capacity of *Phaeocystis antarctica*, which we used here to define the mass-specific light absorption and refractive index for the chemical *classes A2* and *PhM* of POM. We also extend our gratitude to Professor D. Stramski for his valuable advice and friendly comments during this research work.

References

Bandaranayake W. M., 1998, *Mycosporines: are they nature's sunscreens?*, Nat. Prod. Rep., 15 (2), 159–172.

Born M., Wolf E., 1968, *Principles of optics*, Pergamon Press, Oxford, 719 pp., [1973, Russian edn., Nauka, Moskva].

Campbell I. D., Dwek R. A., 1984, *Biological spectroscopy*, Benjamin/Cummings Publ. Comp., Menlo Park, California etc., 404 pp.

Carder K. L., Steward R. G., Harvey G. R., Ortner P. B., 1989, *Marine humic and fulvic acids: their effects on remote sensing of ocean chlorophyll*, Limnol. Oceanogr., 34 (1), 68–81.

Carreto J. I., Carignan M. O., Daleo G., DeMarco S. G., 1990a, *Occurrence of mycosporine-like amino acids in the red-tide dinoflagellate Alexandrium excavatum: UV-photoprotective compounds?*, J. Plankton Res., 12, 909–921.

Carreto J. I., Lutz V. A., DeMarco S. G., Carignan M. O., 1990b, *Influence and wavelength dependence of mycosporine-like aminoacid synthesis in the dinoflagellate Alexandrium excavatum*, [in:] *Toxic marine photoplankton*, E. Graneli, L. Edler, B. Sundstrom & D. M. Anderson (eds.), Elsevier, New York, 275–298.

Favre-Bonvin J., Arpin N., Brevard C., 1976, *Structure de la mycosporine (P310)*, Can. J. Chem., 54, 1105–1113.

Ficek D., Kaczmarek S., Stoń-Egiert J., Woźniak B., Majchrowski R., Dera J., 2004, *Spectra of light absorption by phytoplankton pigments in the Baltic; conclusions to be drawn from a Gaussian analysis of empirical data*, Oceanologia, 46 (4), 533–555.

Filipowicz B., Więckowski W., 1983, *Biochemistry*, Vol. 2, PWN, Warszawa, 624 pp., (in Polish).

Garcia-Pichel F., 1994, *A model for internal self-shading in planktonic organisms and its implications for the usefulness of ultraviolet sunscreens*, Limnol. Oceanogr., 39 (7), 1704–1717.

Grodziński D. M., 1978, *Plant biophysics*, Państ. Wyd. Rol. Leś., Warszawa, 405 pp., (in Polish).

Hayase K., Tsubota K., 1985, *Sedimentary humic acid and fulvic acid as fluorescent organic materials*, Geochim. Cosmochim. Acta, 49, 159–163.

Iturriaga R., Siegel D. A., 1989, *Microphotometric characterization of phytoplankton and detrital absorption propertis in the Sargasso Sea*, Limnol. Oceanogr., 34 (8), 1706–1726.

Jeffrey S. W., Mantoura R. F. C., Bjørnland T., 1997, *Data for the identification of 47 key phytoplankton pigments*, [in:] *Phytoplankton pigments in oceanography: guidelines to modern methods*, S. W. Jeffrey, R. F. C. Mantoura & S. W. Wright (eds.), UNESCO, Paris, 449–559.

Karentz D., McEuen F. S., Land M. C., Dunlap W. C., 1991, *Survey of mycosporine-like aminoacid compounds in Antarctic marine organisms: potential protection from ultraviolet exposure*, Mar. Biol., 108 (1), 157–166.

Kęcki Z., 1993, *Molecular spectroscopy*, PWN, Warszawa, (in Polish).

Majchrowski R., 2001, *Influence of irradiance on the light absorption characteristics of marine phytoplankton*, Diss. and monogr., Pomeranian Pedagogical Univ., Słupsk, 1, 131 pp., (in Polish).

Majchrowski R., Woźniak B., Dera J., Ficek D., Kaczmarek S., Ostrowska M., Koblentz-Mishke O. I., 2000, *Model of the 'in vivo' spectral absorption of algal pigments. Part 2. Practical applications of the model*, Oceanologia, 42 (2), 191–202.

Meyers-Schulte K., Hedges J. I., 1986, *Molecular evidence for a terrestrial component of organic matter dissolved in ocean water*, Nature, 321, 61–63.

Miller N., Carpentier R., 1991, *Energy dissipation and photoprotection mechanisms during chlorophyll photobleaching in thylakoid membranes*, Photochem. Photobio., 54, 465–472.

Moisan T. A., Mitchell B. G., 2001, *UV absorption by mycosporine-like amino acids in Phaeocystis antarctica (Karsten) induced by photosynthetically available radiation*, Mar. Biol., 138 (1), 217–227.

Morel A., Ahn Y. H., 1990, *Optical efficiency factors of free-living marine bacteria: influence of bacterioplankton upon the optical properties and particular organic carbon in oceanic waters*, J. Mar. Res., 48, 145–175.

Nyquist G., 1979, *Investigation of some optical properties of sea water with special reference to lignin sulfonates and humic substances*, Ph. D. thesis, Dept. Analytical and Marine Chemistry, Göteborg Univ., Göteborg, 203 pp.

Pempkowiak J., 1989, *Origin, sources and properties of humic substances in the Baltic Sea*, Ossolineum, Wrocław, 146 pp., (in Polish).

Pope R. M., Fry E. S., 1997, *Absorption spectrum (380–700 nm) of pure water. II. Integrating cavity measurements*, Appl. Optics, 36 (33), 8710–8723.

Romankevich E. A., 1977, *The geochemistry of organic substances in the ocean*, Nauka, Moskva, 256 pp., (in Russian).

Shlyk A. A. (ed.), 1974, *Chlorophyll*, Nauka i Tekhnika, Minsk, 415 pp., (in Russian).

Smith R. C., Baker K. S., 1981, *Optical properties of the clearest natural waters (200–800 nm)*, Appl. Optics, 20 (2), 177–184.

Sogandares F. M., Fry E. S., 1997, *Absorption spectrum 340–640 nm of pure water. I. Photothermal measurements*, Appl. Optics, 36 (33), 8699–8709.

Stramski D., Bricaud A., Morel A., 2001, *Modeling the inherent optical properties of the ocean based on the detailed composition of the planktonic community*, Appl. Optics, 40 (18), 2929–2945.

Stuermer D. H., 1975, *The characterization of humic substances in sea water*, Ph. D. thesis, Mass. Inst. Technol.–Woods Hole Oceanogr. Inst., 163 pp.

Van de Hulst H. C., 1981, *Light scattering by small particles*, Dover Publ., Inc., New York, 470 pp.

Vernet M., Whitehead K., 1996, *Release of ultraviolet-absorbing compounds by the red-tide dinoflagellate Lingulodinium polyedra*, Mar. Biol., 127 (1), 35–44.

Whitehead K., Hedges J. I., 2003, *Electrospray ionization tandem mass spectrometric and electron impact mass spectrometric characterization of mycosporine-like amino acids*, Rapid Commun. Mass Sp., 17 (18), 2133–2138.

Woźniak B., Dera J., Ficek D., Majchrowski R., Kaczmarek S., Ostrowska M., Koblentz-Mishke O. I., 1999, *Modelling the influence of acclimation on the absorption properties of marine phytoplankton*, Oceanologia, 41 (2), 187–210.

Woźniak B., Dera J., Ficek D., Majchrowski R., Kaczmarek S., Ostrowska M., Koblentz-Mishke O. I., 2000, *Model of the 'in vivo' spectral absorption of algal pigments. Part 1. Mathematical apparatus*, Oceanologia, 42 (2), 177–190.

Woźniak B., Woźniak S. B., Tyszka K., Dera J., 2005, *Modelling the light absorption properties of particulate matter forming organic particles suspended in seawater. Part 1. Model description, classification of organic particles, and example spectra of the light absorption coefficient and the imaginary part of the refractive index of particulate matter for phytoplankton cells and phytoplankton-like particles*, Oceanologia, 47 (2), 129–164.

Zepp R., Schlotzhauer P. F., 1981, *Comparison of photochemical behaviour of various humic substances in water: 3. Spectroscopic properties of humic substances*, Chemosphere, 10, 479–486.

Appendix 1

List of symbols and abbreviations denoting the physical quantities used in this paper

Symbol	Denotes	Unit
a	absorption coefficient	m^{-1}
a_{pm}	absorption coefficient of particular (or cellular) matter	m^{-1}
	(or cellular) organic matter	
a_w	absorption coefficient of pure seawater	m^{-1}
a^*	mass-specific absorption coefficient	$m^2\ g^{-1}$
$a^*{}_{air}$	– of light in air (other gas)	$m^2\ g^{-1}$
a^*_{A1}	– of aromatic amino acids (protein fragments)	$m^2\ g^{-1}$
a^*_{A2}	– of mycosporine-like amino acids (MAAs)	$m^2\ g^{-1}$
a^*_{A3}	– of natural proteins	$m^2\ g^{-1}$
a^*_{P1}	– of ocean phytoplankton pigments	$m^2\ g^{-1}$
a^*_{P2}	– of Baltic phytoplankton pigments	$m^2\ g^{-1}$
a^*_N	– of purine and pyridine compounds	$m^2\ g^{-1}$
a^*_L	– of lignins	$m^2\ g^{-1}$
a^*_{H1}	– of Baltic humus	$m^2\ g^{-1}$
a^*_{H2}	– of Atlantic coastal humus	$m^2\ g^{-1}$
a^*_{H3}	– of humus from inland waters	$m^2\ g^{-1}$
a^*_{H4}	– of marine humus	$m^2\ g^{-1}$
a^*_{H5}	– of Sargasso Sea humus	$m^2\ g^{-1}$
a^*_{H6}, a^*_{H7}, a^*_{H8}	– of humus from the Gulf of Mexico	$m^2\ g^{-1}$
a^*_{H9}	– of fulvic acids from Mississippi estuarine waters	$m^2\ g^{-1}$
a^*_{H10}	– of soil humic acids	$m^2\ g^{-1}$
a^*_{H11}	– of soil fulvic acids	$m^2\ g^{-1}$
a^*_{H12}	– of humic acids from bottom sediments	$m^2\ g^{-1}$
a^*_{H13}	– of fulvic acids from bottom sediments containing MAAs	$m^2\ g^{-1}$
a^*_{Ph1}	– of oceanic phytoplankton and phytoplankton-like particles	$m^2\ g^{-1}$
a^*_{Ph2}	– of Baltic phytoplankton and phytoplankton-like particles	$m^2\ g^{-1}$
a^*_{PhM}	– of polar phytoplankton and phytoplankton-like particles	$m^2\ g^{-1}$
a^*_Z	– of zooplankton and zooplankton and/or nekton-like particles	$m^2\ g^{-1}$
a^*_{D1}	– of oceanic DOM-like particles	$m^2\ g^{-1}$
a^*_{D2}	– of Baltic DOM-like particles	$m^2\ g^{-1}$

List of symbols and abbreviations denoting the physical quantities used in this paper (*continued*)

Symbol	Denotes	Unit
a^*_{OM}	– of pure organic material	$\mathrm{m^2\ g^{-1}}$
b	relative buoyancy	dimensionless
C_{acc}	total accessory pigment concentration	mg pigment $\mathrm{m^{-3}}$
C_{air}	average intraparticular concentrations of air	mg pigment $\mathrm{m^{-3}}$
C_b, C_c, C_{PPC}, C_{PSC}	concentrations of chlorophylls b, chlorophylls c, photoprotecting carotenoids, photosynthetic carotenoids	mg pigment $\mathrm{m^{-3}}$
C_i	intraparticular concentration of components (the index i here expresses the number or name of a component in a particle, i.e. a given substance or group of substances)	mg $\mathrm{m^{-3}}$
C_{OM}	average intraparticular (intracellular) concentration of organic matter	g $\mathrm{m^{-3}}$
C_w	average intraparticular (intracellular) concentration of water	g $\mathrm{m^{-3}}$
DOM	dissolved organic matter	
MAAs	mycosporine-like amino acids	
n'	imaginary part of the complex refractive index (non-dimensional absorption coefficient)	dimensionless
n'_p	imaginary part of the complex refractive index for particulate matter (non-dimensional absorption coefficient)	dimensionless
$n'_{p,dry}$	imaginary part of the complex refractive index for dry organic matter	dimensionless
$n'_{p,SS}$	imaginary part of the (absolute or relative) complex refractive index for particulate matter in Sargasso Sea	dimensionless
n'_w	imaginary part of the complex refractive index for water	dimensionless
PAR	photosynthetically available radiation	μEin $\mathrm{m^2\ s^{-1}}$
POM	particulate organic matter	
UV	ultraviolet light	
VIS	visible light	
λ	wavelength of light	nm
ρ_{OM}	density of dry organic matter	g $\mathrm{m^{-3}}$ or kg $\mathrm{m^{-3}}$
ρ_w	density of pure seawater	g $\mathrm{m^{-3}}$ or kg $\mathrm{m^{-3}}$

Appendix 2

The spectra of the mass-specific absorption coefficients of the strongest identified absorbers of UV and/or VIS light

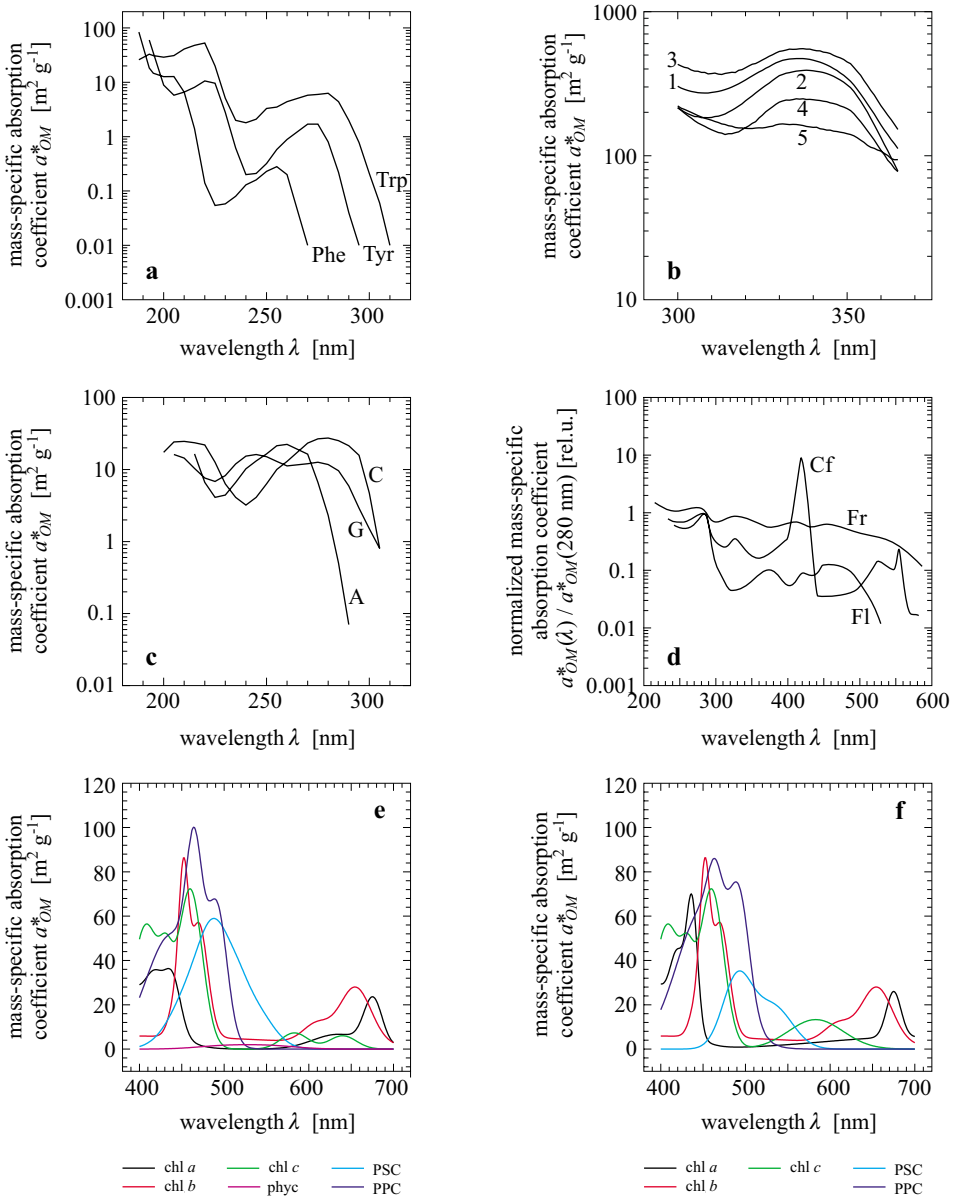

Fig. A2.1. The spectra of the mass-specific absorption coefficients of the strongest identified absorbers of UV and/or VIS in the sea and some of their derivatives: (a) 'aromatic'amino acids: tryptophan (Trp), tyrosine (Tyr) (*continued next page*)

and phenylalanine (Phe) (after data taken from Campbell & Dwek 1984); (b) mycosporine-like amino acids including mycosporine-glycine, shinorine and mycosporine-glycine valine in proportions characteristic of mixtures of these compounds occurring naturally in *Phaeocystis antarctica*, incubated under various irradiance conditions (under PAR irradiance levels of 542, 400, 259, 151 and 85 μEin m^2 s^{-1}, curves 1 to 5 respectively) (these spectra were estimated from empirical data taken from Moisan & Mitchell (2001) and on the basis of private communications from Dr T. A. Moisan); (c) – purine and pyrimidine derivatives – the main constituents of nucleic acids: adenine (A), guanine (G) and cytosine (C) (after data taken from Filipowicz & Więckowski 1983); (d) various conjugated proteins of plant origin: cytochrome (containing haem groups) (Cf), ferredoxin (with iron not bonded via haem groups) (Fe) and flavoproteid (reductose – ferredoxin – NADP) (Fl) (after different authors – data taken from Grodziński (1978)); (e) Baltic phytoplankton pigments: chlorophylls *a* (chl *a*), chlorophylls *b* (chl *b*), chlorophylls *c* (chl *c*), phycobilins (phyc), photosynthetic carotenoids (PSC), and photoprotecting carotenoids (PPC) (after data taken from Ficek et al. 2004); and (f) ocean phytoplankton pigments (symbols as described in panel (e)) (after data taken from Woźniak et al. 1999)

Fig. A2.1 shows the spectra of the mass-specific absorption coefficients of light for selected compounds from a few groups of organic substances identified as the strongest absorbers of UV-VIS light. These spectra were used in this paper to determine the resultant absorption properties of the organic matter contained in many of the model chemical classes of POM (only particles containing one organic component). All the absorption spectra in Fig. A2.1 were determined experimentally by ourselves or were taken from the work of other authors (acknowledgements in the figure caption).

Appendix 3

The light absorption capacity of *Phaeocystis antarctica* as the basis for defining the mass-specific light absorption for organic matter from the chemical *classes A2* and *PhM* of POM

Mycosporine-like amino acids (MAAs) strongly absorb UV radiation in the 300–370 nm region. Their structures and chemical properties were described relatively recently (see e.g. Favre-Bonvin et al. 1976, Bandaranayake 1998, Whitehead & Hedges 2003). These substances are synthesised by various species of marine algae (Carreto et al. 1990a,b, Karentz et al. 1991, Miller & Carpentier 1991). Their presence is especially characteristic of the phytoplankton from polar regions, which are exposed to high doses of UV radiation. Several studies (e.g. Garcia-Pichel 1994, Vernet & Whitehead 1996) have suggested that MAAs act as natural sunscreens to UV radiation and as such should be considered photoprotective; this is endorsed by a number of empirical circumstances. This has also been confirmed indirectly during detailed laboratory studies by, for example, Moisan & Mitchell (2001). These researchers have shown that the MAAs (in particular, mycosporine-glycine, shinorine and mycosporine-glycine valine) contained in *Phaeocystis antarctica* behave in the same way as photoprotecting carotenoids and are proportional to the light intensity under which the cultures in question were incubated.

Recapitulating, then, we assumed that under certain conditions in the sea (e.g. in polar regions with an elevated level of UV), there may occur phytoplankton species with high levels of MAAs, higher than is normally the case in most natural phytoplankton populations. That is why we have extended the list of model chemical classes of POM to include the following two classes of particles: polar phytoplankton and phytoplankton-like particles (*class PhM*) and particles made up of MAAs (*class A2*), which can come into existence upon the disintegration of *PhM* particles. Hence, to determine the mass-specific light absorption coefficients $a^*_{\mathrm{OM}}(\lambda)$ for these two chemical classes of particle, i.e. for particles made up of MAAs ($a^*_{A2}(\lambda) = a^*_{MAAs}(\lambda)$) and for polar phytoplankton and polar phytoplankton-like particles ($a^*_{PhM}(\lambda)$), in section 2 of this paper, we made use of the empirical data on the light absorption capacity of such natural particles obtained by Moisan & Mitchell (2001). Dr Moisan kindly supplied us with the relevant set of data, including some not cited in the paper just mentioned. The set contained a variety of empirical data, including optical data on the total absorption of light by phytoplankton and by its photosynthetic pigments. Covering not only cellular in vivo absorption but also absorption by unpackaged cellular material, the data applies to cultures of colonial *P. antarctica* incubated under a range of irradiance conditions. In the present paper, we used five sets of these data referring to the following properties of these algae and for five different levels of *PAR*: 542, 400, 259, 151 and 85 μEin m^2 s^{-1}:

- $a^*_{ph}(\lambda)$ [m^2 (mg chl a)$^{-1}$] and $a^*_{ps}(\lambda)$ [m^2 (mg chl a)$^{-1}$] – the respective spectra of the chlorophyll-specific absorption of light of unpackaged cellular material by all the components of phytoplankton (a^*_{ph}) and by photosynthetic pigments (a^*_{ps}), for the spectral range from 300 to 700 nm;

- d_{MAAs}/chl, d_1/chl, d_2/chl, d_3/chl – the respective cellular ratios of the combined mass of all MAAs (d_{MAAs}) and their three principal components (1-mycosporine-glycine (d_1), 2-shinorine (d_2) and 3-mycosporine-glycine valine (d_3)), to the mass of chlorophyll a (chl), expressed in [nmol MAAs per μg chl a];

- d_{MAAs}/C_{org} – the ratio of the MAA content to the organic carbon content in a cell (C_{org}), expressed in [nmol MAAs per μg C].

Employing the above data and assuming that in the 300–365 nm spectral interval the absorption of light by MAAs and to some extent also by photosynthetic pigments is far greater than that by the other substances contained in a phytoplankton cell, the spectral mass-specific light absorption only by matter containing MAAs was estimated as the difference between the spectra of $a^*_{ph}(\lambda)$ and $a^*_{ps}(\lambda)$. The spectra of a^*_{MAAs} were then calculated from the following relationship:

$$a^*_{A2}(\lambda) \,=\, a^*_{MAAs}(\lambda)\,\left[\mathrm{m}^2\ \mathrm{g}^{-1}\right] \,=\, k_1(\overline{mw}_{MAAs})^{-1}\left(\frac{d_{MAAs}}{\mathrm{chl}}\right)^{-1}\left[a^*_{ph}(\lambda)\,-\,a^*_{ps}(\lambda)\right], \tag{A3.1}$$

where $k_1 = 10^6$, and is a coefficient resulting from the conversion of units; $\overline{mw}_{MAAs}$ [g mol^{-1}] is the mean molar weight of a mixture of compounds from the MAA group, dependent on the individual cellular levels of the various amino acids and on their molar weights mw_i, in line with the relationship:

$$\overline{mw}_{MAAs} = (d_{MAAs})^{-1}\Sigma_i(d_{MAAs,i}\,mw_i), \tag{A3.2}$$

where mw_i is equal to 243, 332 and 344 g mol^{-1}, for mycosporine-glycine, shinorine and mycosporine-glycine valine respectively.

Determined for five natural mixtures of MAAs at different irradiances, these spectra are illustrated in Fig. A2.1b in Appendix 2. The spectrum $a^*_{A2}(\lambda)$, which was obtained by averaging these five spectra, is assumed in this paper to represent the model chemical *class A2*; it is given as a number in Table 2 (column 3) and is illustrated in Fig. 1a (curve A2).

Similar spectra of mass-specific light absorption coefficient by the combined organic matter in phytoplankton cells were determined on the basis of the spectrum of $a^*_{ps}(\lambda)$, according to the equation

$$a^*_{PhM}(\lambda)\,\left[\mathrm{m}^2\ \mathrm{g}^{-1}\right] = 0.5\,k_2\left(\frac{d_{MAAs}}{C_{org}}\right)\left(\frac{d_{MAAs}}{\mathrm{chl}}\right)^{-1} a^*_{ph}(\lambda), \tag{A3.3}$$

where $k_2 = 10^3$, and is a coefficient resulting from the conversion of units; the factor 0.5 emerges from the approximate assumption that the overall mass of organic matter in a cell is about twice as high as the mass of carbon it contains.

Equation (A3.3) was used to determine five approximate spectra of the mass-specific absorption coefficients of light by cellular matter in cultures of *P. antarctica* incubated under different irradiance conditions. On the other hand, we assumed the mean spectrum of $a^*_{PhM}(\lambda)$ (see Fig. 1d, curve PhM), the average of the above five spectra, to be representative of the *class PhM*, i.e. polar phytoplankton and polar phytoplankton-like particles.

Appendix 4

The biochemical composition of marine organisms

Marine organisms are the chief source from which fractions of POM in the sea are derived directly or indirectly. A considerable proportion of these organisms, which are very small in size, also makes up the living part of these POM fractions. In the present paper, therefore, we took into account the typical biochemical compositions of these organisms when establishing the compositions of organic matter and the overall composition of organic and inorganic matter of the model particles, which we placed in various model chemical classes and physical types. These compositions also suggested themselves when it came to dividing POM into two groups: (1) commonly occurring dry or moderately hydrated particles, and (2) strongly hydrated particles. The data applying to these compositions are set out in Table A4.1. This gives the typical proportions by weight (as a percentage) for the principal groups of organisms living in the sea (phytoplankton, phytobenthos, zooplankton, zoobenthos and nekton) with respect to: the combined (wet) matter in these organisms, divided into organic matter, water, other inorganic substances (contained in ash); and the organic matter contained in these organisms divided into two groups: all simple and complex proteins and their components (amino acids, peptides and proteids), and other organic substances.

Having established these proportions, we then based the biochemical composition of marine organisms on data taken from the monograph by Romankevich (1977), which summarises the research results of variousauthors.

Table A4.1. The biochemical composition of marine organisms

Organisms	Relative content as a % of the mass				
	Combined (wet) matter			Organic matter	
	water	organic matter	other inorganic matter (ash)	proteins	other compounds
phytoplankton	80	11	9	55	45
phytobenthos	80	15	5	20	80
zooplankton	80	18	2	67	33
zoobenthos	63	14	23	71	29
nekton	73	24	3	78	22